

Export fluxes in  
a naturally fertilized  
area – Part 2

M. Rembauville et al.

# Export fluxes in a naturally fertilized area of the Southern Ocean, the Kerguelen Plateau: ecological vectors of carbon and biogenic silica to depth (Part 2)

M. Rembauville<sup>1,2</sup>, S. Blain<sup>1,2</sup>, L. Armand<sup>3</sup>, B. Quéguiner<sup>4</sup>, and I. Salter<sup>1,2,5</sup>

<sup>1</sup>Sorbonne Universités, UPMC Univ Paris 06, UMR 7621, LOMIC, Observatoire Océanologique, Banyuls-sur-Mer, France

<sup>2</sup>CNRS, UMR 7621, LOMIC, Observatoire Océanologique, Banyuls-sur-Mer, France

<sup>3</sup>Department of Biological Sciences and Climate Futures, Macquarie University, New South Wales, Australia

<sup>4</sup>Aix-Marseille Université Université de Toulon, CNRS/INSU, IRD, MOI, UM 110, Marseille, France

<sup>5</sup>Alfred-Wegener-Institute for Polar and Marine research, Bremerhaven, Germany

Received: 7 November 2014 – Accepted: 13 November 2014 – Published: 10 December 2014

Correspondence to: M. Rembauville (rembauville@obs-banyuls.fr)

Published by Copernicus Publications on behalf of the European Geosciences Union.

Title Page

Abstract

Introduction

Conclusions

References

Tables

Figures



Back

Close

Full Screen / Esc

Printer-friendly Version

Interactive Discussion



## Abstract

The chemical (particulate organic carbon and nitrogen, biogenic silica) and biological (diatoms and faecal pellets) composition of the material exported to a moored sediment trap located under the winter mixed layer of the naturally-fertilized Kerguelen Plateau in the Southern Ocean was studied over an annual cycle. Despite iron availability in spring, the annual particulate organic carbon (POC) export ( $98.2 \text{ mmol m}^{-2}$ ) at 289 m was low but annual biogenic silica export was significant ( $114 \text{ mmol m}^{-2}$ ). This feature was related to the abundance of empty diatom frustules and the ratio of full:empty cell exerted a first order control in BSi:POC export stoichiometry of biological pump. *Chaetoceros Hyalochaete* spp. and *Thalassiosira antarctica* resting spores were found to be responsible for more than 60 % of the annual POC that occurred during two very short export events (< 14 days in spring-summer) representing the majority of captured export. Low diatom fluxes were observed over the remainder of the year. Faecal pellet contribution to annual carbon flux was low (34 %) and reached its seasonal maximum in autumn and winter (> 80 %). The seasonal progression of faecal pellet types revealed a clear transition from small spherical shapes (small copepods) in spring, larger cylindrical and ellipsoid shapes in summer (euphausiids and large copepods) and finally large tabular shapes (salps) in autumn and winter. We propose that in this High Biomass, Low Export (HBLE) environment, small, highly silicified, fast-sinking resting spores are able to bypass the high grazing pressure and efficient carbon transfer to higher trophic levels that are responsible for the low fluxes observed the during the remainder of the year. Our study also provides a statistical framework linking the ecological succession of diatom and zooplankton communities to the seasonality of carbon and silicon export within an iron-fertilized bloom region in the Southern Ocean.

## Export fluxes in a naturally fertilized area – Part 2

M. Rembauville et al.

[Title Page](#)

[Abstract](#)

[Introduction](#)

[Conclusions](#)

[References](#)

[Tables](#)

[Figures](#)



[Back](#)

[Close](#)

[Full Screen / Esc](#)

[Printer-friendly Version](#)

[Interactive Discussion](#)



## 1 Introduction

The Southern Ocean is the place of exposure of old upwelled waters to the atmosphere and the formation of modal waters, thereby ventilating an important part of the global Ocean and playing a central role in distributing heat, carbon and nutrients in the global Ocean (Sarmiento et al., 2004; Takahashi et al., 2012; Sallée et al., 2012). Silicon trapping occurs in the Southern Ocean because silicon is stripped out of the euphotic zone more efficiently than phosphorous and nitrogen (Holzer et al., 2013). It is generally acknowledged that regional variations in plankton community structure are responsible for variations in nutrient stoichiometry in the Southern Ocean (Jin et al., 2006; Weber and Deutsch, 2010) and that the biological pump is a central process regulating this stoichiometry (Ragueneau et al., 2006; Salter et al., 2012; Primeau et al., 2013). These characteristics emphasize the importance of biological processes in the Southern Ocean waters for the availability of silicic acid and nitrate (Sarmiento et al., 2004; Dutkiewicz et al., 2005) as well as phosphate (Primeau et al., 2013) at lower latitudes, thereby regulating part of the productivity of the global Ocean. It has been proposed that change in the uptake ratio of silicate and nitrate by Southern Ocean phytoplankton in response to increased iron availability during the Last Glacial Maximum could have played a substantial role in varying atmospheric CO<sub>2</sub> (Brzezinski et al., 2002; Matsumoto et al., 2002).

Primary production in the Southern Ocean is regulated by macro- and micronutrients availability (Martin et al., 1990; Moore et al., 2001, 2013; Nelson et al., 2001) and light-mixing regime (Venables and Moore, 2010; Blain et al., 2013). The complex interaction of these factors introduces strong spatial heterogeneity in the distribution of primary producer biomass (Arrigo et al., 1998; Thomalla et al., 2011). In particular, High Nutrient, Low Chlorophyll (HNLC) areas in the open ocean contrast strongly with highly productive, naturally fertilized, blooms located downstream of island systems such as the Kerguelen Plateau (Blain et al., 2001, 2007), Crozet Islands (Pollard et al., 2002) and South Georgia (Park et al., 2010; Tarling et al., 2012). The diatom-dominated phy-

### Export fluxes in a naturally fertilized area – Part 2

M. Rembauville et al.

Title Page

Abstract

Introduction

Conclusions

References

Tables

Figures



Back

Close

Full Screen / Esc

Printer-friendly Version

Interactive Discussion



## Export fluxes in a naturally fertilized area – Part 2

M. Rembauville et al.

[Title Page](#)

[Abstract](#)

[Introduction](#)

[Conclusions](#)

[References](#)

[Tables](#)

[Figures](#)



[Back](#)

[Close](#)

[Full Screen / Esc](#)

[Printer-friendly Version](#)

[Interactive Discussion](#)



toplankton blooms characteristic of these island systems are the product of multiple environmental conditions favorable for their rapid growth (Quéguiner, 2013), which appear to promote POC export from the mixed layer (Nelson et al., 1995; Buesseler, 1998). However the ecological traits of certain species can impact the BSi:POC export stoichiometry (Crawford, 1995; Salter et al., 2012), and may therefore control the biogeochemical function of a particular region of the Southern Ocean (Smetacek et al., 2004; Assmy et al., 2013).

Among the numerous ecological characteristics of plankton communities, algal aggregation (Jackson et al., 2005; Burd and Jackson, 2009), mesozooplankton faecal pellet (Lampitt et al., 1990; Wilson et al., 2008, 2013), vertical migrations of zooplankton and mesopelagic fish (Jackson and Burd, 2001; Steinberg et al., 2002; Davison et al., 2013), radiolarian faecal pellet (Lampitt et al., 2009), and diatom resting spore formation (Salter et al., 2012; Rynearson et al., 2013) have all been highlighted as efficient vectors of carbon export out of the surface mixed layer. The challenge in describing the principal ecological processes regulating POC export fluxes is the requirement to have direct access to sinking particles. Many of the processes described occur in the upper layers of the ocean, where circulation can strongly influence the reliability of sediment trap collections (Baker et al., 1988; Buesseler et al., 2007). Short term deployments of free drifting sediment traps can be an efficient solution to minimize the hydrodynamic bias (Buesseler et al., 2000; Lampitt et al., 2008) but spatial and temporal decoupling of production and export needs to be considered (Salter et al., 2007; Rynearson et al., 2013). In regions characterized by relatively weak circulation, moored sediment trap observations in areas of naturally fertilized production can track temporal succession of exported material from long-term (several month) blooms (Westberry et al., 2013). Such an approach can partially resolve how ecological processes in plankton communities regulate POC and biomineral export out of the mixed layer, although selective processes during export may modify original surface features.

The central Kerguelen Plateau is a good environment to study the ecological vectors of export with sediment traps due to the naturally fertilized recurrent bloom (Blain

## Export fluxes in a naturally fertilized area – Part 2

M. Rembauville et al.

Title Page

Abstract

Introduction

Conclusions

References

Tables

Figures



Back

Close

Full Screen / Esc

Printer-friendly Version

Interactive Discussion



et al., 2007) and shallow bathymetry that breaks the strong Antarctic Circumpolar Current flow (Park et al., 2008, 2014). As reported in the companion paper (Rembauville et al., 2014), annual POC export measured by the sediment trap deployment at 289 m beneath the southeastern iron-fertilized Kerguelen bloom is  $98 \pm 4 \text{ mmol m}^{-2} \text{ yr}^{-1}$ . This downward flux of carbon may account for as little as  $\sim 1.5 \%$  of seasonal net community carbon production ( $6.6 \pm 2.2 \text{ mol m}^{-2}$ , Jouandet et al., 2008) and  $< 2 \%$  of seasonally integrated POC export estimated at 200 m from a dissolved inorganic carbon budget ( $5.1 \text{ mol C m}^{-2}$ ; Blain et al., 2007). A comparison of POC fluxes over short-term intervals ( $< 1$  month) from a wide variety of approaches revealed similar reductions in POC flux between 200 and 300 m during spring and summer (Rembauville et al., 2014). Such a rapid attenuation of flux appears to be inconsistent with microbial remineralization of settling particles (Rembauville et al., 2014). Previously, we have suggested the role of higher trophic levels (mesozooplankton and mesopelagic fish) feeding at the base of the mixed layer as an explanation for the “High Biomass, Low Export” (HBLE, Lam and Bishop, 2007) environment characterizing the productive Kerguelen Plateau. HBLE status appears to be a common feature of other productive sites of the Southern Ocean (Lam and Bishop, 2007; Ebersbach et al., 2011; Lam et al., 2011; Maiti et al., 2013). Describing the temporal succession of POC and BSi flux vectors from the Kerguelen Plateau is of interest to increase our understanding of the ecological processes characterizing HBLE environments. In particular, phytoplankton community composition and faecal pellet fluxes may be a significant component of particles exported from the Kerguelen Plateau.

Several studies have described diatom fluxes from sediment trap records in the Southern Ocean (Leventer and Dunbar, 1987; Fischer et al., 1988, 2002; Abelmann and Gersonde, 1991; Leventer, 1991; Gersonde and Zielinski, 2000; PilskaIn et al., 2004; Ichinomiya et al., 2008; Salter et al., 2012; Grigorov et al., 2014; Rigual-Hernandez et al., 2014). Highest diatom fluxes ( $> 10^9 \text{ cells m}^{-2} \text{ d}^{-1}$ ) are observed in the Seasonal Ice Zone (SIZ) near Prydz Bay and Adélie Land and are dominated by *Fragilariopsis kerguelensis* and small species of *Fragilariopsis curta* and *Fragilariopsis*

*cylindrus* (Suzuki et al., 2001; Pilskaln et al., 2004). These high fluxes occur in spring and are associated with the melting of sea ice. Changes in light availability and melt water input appear to establish favorable conditions for the production and export of phytoplankton cells (Romero and Armand, 2010). In the Permanently Open Ocean Zone (POOZ), diatom fluxes are two orders of magnitude lower  $\sim 10^7$  cell m<sup>-2</sup> d<sup>-1</sup> (Abelmann and Gersonde, 1991; Salter et al., 2012; Grigorov et al., 2014) and typically represented by *F. kerguelensis* and *Thalassionema nitzschioides*, except in the naturally fertilized waters downstream of the Crozet Plateau where resting spores of *Eucampia antarctica* var. *antarctica* dominate the diatom export assemblage (Salter et al., 2012).

Other studies have reported the faecal pellet contribution to POC fluxes in the Southern Ocean (Dunbar, 1984; Wefer et al., 1988, 1990; Wefer and Fisher, 1991; Dubischar and Bathmann, 2002; Suzuki et al., 2001, 2003; Accornero and Gowing, 2003; Schnack-Schiel and Isla, 2005; Gleiber et al., 2012) with a particular emphasis on shelf processes where faecal pellet contribution to POC flux is higher than in the oceanic regions (Wefer et al., 1990; Wefer and Fischer, 1991; Schnack-Schiel and Isla, 2005). In the Ross Sea there is a northward decreasing contribution of faecal pellets to carbon flux of 59, 38 and 15% for southern, central and northern areas reported from 235 m sediment traps deployments (Schnack-Schiel and Isla, 2005). Faecal pellets in the Ross Sea, are generally represented by larger shapes with only 2 to 3% of them present as small spherical or ellipsoid shapes and total faecal pellet flux is slightly higher than 10<sup>3</sup> pellet m<sup>-2</sup> d<sup>-1</sup>. High faecal pellet contribution to carbon fluxes (> 90%) has been observed in the Bransfield Strait and the Marginal Ice Zone of the Scotia Sea, and linked to the abundance of the Antarctic krill *Euphausia superba*, resulting in maximum recorded fluxes of  $> 5 \times 10^5$  pellets m<sup>-2</sup> d<sup>-1</sup> (Bodungen, 1986; von Bodungen et al., 1987; Wefer et al., 1988). The strong contribution of krill faecal pellets to carbon flux in the western Antarctic Peninsula was confirmed over several years of observations, with the highest contributions to carbon flux succeeding the phytoplankton bloom in January and February (Gleiber et al., 2012).

## Export fluxes in a naturally fertilized area – Part 2

M. Rembauville et al.

[Title Page](#)[Abstract](#)[Introduction](#)[Conclusions](#)[References](#)[Tables](#)[Figures](#)[Back](#)[Close](#)[Full Screen / Esc](#)[Printer-friendly Version](#)[Interactive Discussion](#)

In the present study, particulate material exported from the mixed layer in the naturally fertilized Permanently Open Ocean Zone (POOZ) of the Kerguelen Plateau is described from an annual sediment trap mooring. To develop our understanding of seasonal variability in the ecological flux vectors and particle biogeochemistry we investigate the link between the chemical (POC, PON, BSi) and biological (diatom species and faecal pellet types) components of exported particles. Furthermore, we advance the limitations of previous studies by explicitly distinguishing full and empty diatom cells in the exported material and thereby determine species-specific roles for carbon and silica export.

## 2 Materials and methods

As part of the multidisciplinary research program KEOPS2 a moored sediment trap (Technicap PPS3) was deployed at 289 m at the representative bloom station A3 (50°38.3' S–72°02.6' E) for a period of 321 days (21 October 2011 to 7 September 2012). The sediment trap mooring was located within an iron-fertilized bloom site on the southern part of the Kerguelen Plateau (Blain et al., 2007). Details of sediment trap design, hydrological conditions and deployment conditions are provided in a companion paper (Rembauville et al., 2014). The cup rotation dates of the sediment trap are listed in Table 1.

### 2.1 Sediment trap sample processing

Details of sediment trap sample retrieval and processing methods have been presented in Rembauville et al. (2014). In brief, swimmers were removed and classified from samples under a dissecting microscope. The samples were quantitatively divided into 8 aliquots using a Jencons peristaltic splitter with a precision of ~2.9%. Particulate material was separated from the overlying preservative fluid by a centrifugation and freeze-drying procedure.

## Export fluxes in a naturally fertilized area – Part 2

M. Rembauville et al.

Title Page

Abstract

Introduction

Conclusions

References

Tables

Figures



Back

Close

Full Screen / Esc

Printer-friendly Version

Interactive Discussion



## 2.2 Chemical measurements

POC and PON analyses have been previously described in Rembauville et al. (2014). In summary, 3 to 5 mg of freeze-dried material were weighed directly into pre-combusted (450 °C, 24 h) silver cups and decarbonated through the addition of 2N HCl. Samples were dried overnight at 50 °C and POC and PON were measured with a CHN analyzer (Perkin Elmer 2400 Series II CHNS/O Elemental Analyzer) calibrated with glycine. Samples were analyzed in triplicate with an analytical precision of less than 0.3 %.

For the analysis of biogenic silica (BSi) and lithogenic silica (LSi), 2 to 8 mg of freeze-dried material were weighed (Sartorius precision balance, precision  $10^{-4}$  g) and placed into falcon tubes. The extraction of silicon from biogenic and lithogenic particle phases was performed following the Ragueneau et al. (2005) triple NaOH/HF extraction procedure. Silicic acid ( $\text{Si}(\text{OH})_4$ ) resulting from NaOH extractions was measured automatically on a Skalar 5100 autoanalyzer whereas  $\text{Si}(\text{OH})_4$  resulting from HF extraction was measured manually on a Milton Roy Spectronic 401 spectrophotometer.  $\text{Si}(\text{OH})_4$  acid analyses were performed colorimetrically following Aminot and Kerouel (2007). Standards for the analysis of samples from the HF extraction were prepared in an HF/ $\text{H}_3\text{BO}_4$  matrix, ensuring the use of an appropriate calibration factor that differs from Milli-Q water. The contribution of LSi to the first leaching was determined by using Si : Al ratios from a second leaching step (Ragueneau et al., 2005). Aluminum concentrations were measured by spectrophotometry (Howard et al., 1986). The triple extraction procedure is designed for samples with a BSi content  $< 10 \mu\text{mol}$ . For some samples (cup #3, #4, #6, #7, #8, #9 and #10) the Si : Al molar ratio in the second leachate was high ( $> 10$ ) indicating the incomplete dissolution of BSi. For these samples it was not possible to use Si : Al ratios to correct for LSi leaching. A crustal Si : Al mass ratio of 3.74 (Taylor and McClennan, 1986) was used instead and applied to all the samples for consistency. Precision (estimated from measurement of 25 independent samples) was  $13 \text{ nmol mg}^{-1}$ , which represents  $< 1 \%$  of the BSi content in all samples and 14 % of the

BGD

11, 17089–17150, 2014

### Export fluxes in a naturally fertilized area – Part 2

M. Rembauville et al.

Title Page

Abstract

Introduction

Conclusions

References

Tables

Figures



Back

Close

Full Screen / Esc

Printer-friendly Version

Interactive Discussion



mean LSi content. Blank triplicates from each extraction were lower than the detection limit. BSi results from this method were compared to the kinetic method from DeMaster (1981). There was an excellent agreement between the two methods (Spearman rank correlation,  $n = 12$ ,  $p < 0.001$ ,  $BSi_{kinetic} = 1.03 BSi_{triple\ extraction} - 0.08$ , data not shown)

In order to correct for the dissolution of BSi during deployment and storage,  $Si(OH)_4$  excess was analyzed in the overlying preservative solution. Particulate BSi fluxes were corrected for dissolution assuming that excess silicic acid originated only from the dissolution of BSi phases.  $Si(OH)_4$  excess was always  $< 10\%$  of total (dissolved + particulate) Si concentrations. Error propagation for POC, PON, BSi fluxes and molar ratios were calculated as the quadratic sum of the relative error from triplicate measurements of each variable.

### 2.3 Diatom identification, fluxes and biomass

Many sediment trap studies reporting diatom fluxes in the Southern Ocean use a micropaleontological protocol that oxidizes organic material ( $KMnO_4$ ,  $HCl$ ,  $H_2O_2$ ) thereby facilitating the observation of diatom frustules (see Romero et al., 1999, 2000 for a description). In the present manuscript, our specific aim was to separately enumerate full and empty diatom cells captured by the sediment trap to identify key carbon or silicon exporters amongst the diatom species. We therefore used a biological method following a similar protocol to that of Salter et al. (2007, 2012). To prepare samples for counting, 2 mL of a gently homogenized 1/8 wet aliquot were diluted in a total volume of 20 mL of artificial seawater ( $S = 34$ ). In order to minimize the exclusion and/or breaking of large or elongated diatom frustules (e.g. *Thalassiothrix antarctica*), the pipette tip used for sub-sampling was modified to increase the tip aperture to  $> 2$  mm. The diluted and homogenized sample was placed in a Sedgewick–Rafter counting chamber (Pyser SGE S52, 1 mL chamber volume). Each sample was observed under an inverted microscope (Olympus IX71) with phase contrast at 200x and 400x magnification. Diatom enumeration and identification was made from one quarter to one half of the counting

**BGD**

11, 17089–17150, 2014

## Export fluxes in a naturally fertilized area – Part 2

M. Rembauville et al.

Title Page

Abstract

Introduction

Conclusions

References

Tables

Figures



Back

Close

Full Screen / Esc

Printer-friendly Version

Interactive Discussion



chamber (depending on cell abundance) following the taxonomic description in Hasle and Syvertsen (1997).

Due to the lower magnification used and preserved cell contents sometimes obscuring taxonomic features on the valve face, taxonomic identification to the species level was occasionally difficult and necessitated the categorizing of diatom species to genus or taxa groupings in the following manner: *Chaetoceros* species of the subgenus *Hyalochaete* resting spores (CRS) were not differentiated into species or morphotypes but were counted separately from the vegetative cells; *Fragilariopsis separanda* and *Fragilarsiopsis rhombica* were grouped as *Fragilariopsis separanda/rhombica*; *Membraneis imposter* and *Membraneis challengerii* and species of the genera *Banquisia* and *Manguinea* were denominated as *Membraneis* spp. (Armand et al., 2008a); diatoms of the genus *Haslea* and *Pleurosigma* were grouped as *Pleurosigma* spp.; all *Pseudo-nitzschia* species encountered were grouped as *Pseudo-nitzschia* spp.; *Rhizosolenia antennata* and *Rhizosolenia styliiformis* were grouped as *Rhizosolenia antenanta/styliiformis*; large and rare *Thalassiosira oliverana* and *Thalassiosira tumida* were grouped as *Thalassiosira* spp.; *Thalassiosira antarctica* resting spores (TRS) were identified separately from the vegetative cells; small centric diatoms (< 20 µm) represented by *Thalassiosira gracilis* and other *Thalassiosira* species were designated as Small centrics (< 20 µm); and finally large and rare centrics including *Azpeitia tabularis*, *Coscinodiscus* spp. and *Actinocyclus curvatulus* were grouped as Large centrics (> 20 µm). Full and empty frustules of each species or taxa grouping were distinguished and enumerated separately. The cell flux for each diatom species or taxa grouping was calculated according to Eq. (1):

$$Cell\ flux = N_{diat} \times d \times 8 \times V_{cup} \times \frac{1}{0.125} \times \frac{1}{days} \times chamber\ fraction \quad (1)$$

Where *Cell flux* is in cells m<sup>-2</sup> d<sup>-1</sup>, *N<sub>diat</sub>* is the number of cells enumerated for each diatom classification, *d* is the dilution factor from the original wet aliquot, 8 is the total number of wet aliquots comprising one sample cup, *V<sub>cup</sub>* is the volume of each wet

## BGD

11, 17089–17150, 2014

### Export fluxes in a naturally fertilized area – Part 2

M. Rembauville et al.

Title Page

Abstract

Introduction

Conclusions

References

Tables

Figures



Back

Close

Full Screen / Esc

Printer-friendly Version

Interactive Discussion



aliquot, 0.125 is the Technicap PPS/3 sediment trap collecting area (m<sup>2</sup>), *days* is the collecting period, *chamber fraction* is the surface fraction of the counting chamber that was observed (one quarter or one half).

We directly compared the micropaleontological and biological counting techniques in our sediment trap samples and noted the loss of several species (*Chaetoceros decipiens/dichaeta*, *Corethron pennatum/inerme*, *Guinardia cylindrus* and *Rhizosolenia chunii*) with the micropaleontological technique. We attribute this to the aggressive chemical oxidation techniques used to “clean” the samples which appears to selectively destroy/dissolve certain frustules. For the species that were commonly observed by both techniques, total valve flux was in good agreement (Spearman rank correlation,  $n = 12$ ,  $\rho = 0.91$ ,  $p < 0.001$ , data not shown) although consistently lower with the micropaleontological technique, probably due to the loss of certain frustules described above. Full details of this method comparison are in preparation for a separate submission.

Biomass calculations for both *Chaetoceros Hyalochaete* resting spores (CRS) and *Thalassiosira antarctica* resting spores (TRS) were determined from > 50 randomly selected complete resting spores observed in splits from cups #4 to #11. Morphometric measurements (perivalvar and apical axis) were made using the Fiji image processing package (available at <http://fiji.sc/Fiji>) on images taken with an Olympus DP71 camera. Cell volumes followed appropriate shape designated calculations from Hillebrand et al. (1999) (Table 2). The cell volume coefficient of variation was 46 and 54 % for CRS and TRS, respectively. CRS carbon content was estimated from the derived cell volume using the volume to carbon relationship of 0.039 pmol C  $\mu\text{m}^{-3}$  established from the resting spore of *Chaetoceros pseudocurvisetus* (Kuwata et al., 1993), leading to a mean value of 227 pgC cell<sup>-1</sup> (Table 2). There is currently no volume to carbon relationship for *Thalassiosira antarctica* resting spores described in the literature, therefore, the allometric relationship for vegetative diatoms (Menden-Deuer and Lessard, 2000) was used to calculate our TRS carbon content, giving a mean value of 1428 pgC cell<sup>-1</sup>

## BGD

11, 17089–17150, 2014

### Export fluxes in a naturally fertilized area – Part 2

M. Rembauville et al.

Title Page

Abstract

Introduction

Conclusions

References

Tables

Figures



Back

Close

Full Screen / Esc

Printer-friendly Version

Interactive Discussion



(Table 2). Resting spores fluxes were converted to carbon fluxes as follows:

$$C \text{ flux}_{(\text{CRS})} = \frac{\text{CRS flux} \times 227 \text{ pg C cell}^{-1}}{M_{12\text{C}} \times 10^9} \quad (2)$$

$$C \text{ flux}_{(\text{TRS})} = \frac{\text{TRS flux} \times 1428 \text{ pg C cell}^{-1}}{M_{12\text{C}} \times 10^9} \quad (3)$$

where  $C \text{ flux}_{(\text{RS})}$  is the carbon flux carried by each resting spore ( $\text{mmol C m}^{-2} \text{ d}^{-1}$ ),  $RS \text{ flux}$  is the full spore numerical flux ( $\text{cell m}^{-2} \text{ d}^{-1}$ ),  $M_{12\text{C}}$  is the molecular weight of  $^{12}\text{C}$  ( $12 \text{ g mol}^{-1}$ ) and  $10^9$  is a conversion factor from pmol to mmol. Other diatoms species that contributed to more than 1% of total cell flux (*E. antarctica* var. *antarctica*, *Fragilariopsis kerguelensis*, *Fragilariopsis separanda/rhombica*, *Pseudo-nitzschia* spp. and *Thalassionema nitzschioides* spp.) were converted to carbon flux using cell-specific carbon content for diatoms communities of the Kerguelen Plateau from Cornet-Barthaux et al. (2007).

## 2.4 Faecal pellet composition and fluxes

To enumerate faecal pellets an entire 1/8 aliquot of each sample cup was placed in a gridded petri dish and observed under a stereomicroscope (Zeiss Discovery V20) coupled to a camera (Zeiss Axiocam ERc5s) at 10x magnification. Photographic images ( $2560 \times 1920$  pixels,  $3.49 \mu\text{m pixel}^{-1}$ ) covering the entire surface of the petri dish were acquired. Following Wilson et al. (2013), faecal pellets were classified into five types according to their shape: spherical, ovoid, cylindrical, ellipsoid and tabular. The flux of each faecal pellet class ( $\text{nb m}^{-2} \text{ d}^{-1}$ ) was calculated as follows:

$$\text{Faecal pellet flux} = N_{\text{FP}} \times 8 \times \frac{1}{0.125} \times \frac{1}{\text{days}} \quad (4)$$

where  $N_{\text{FP}}$  is the number of pellets within each class observed in the 1/8th aliquot. The other constants are as described in Eq. (1). Individual measurements of the major and

## Export fluxes in a naturally fertilized area – Part 2

M. Rembauville et al.

Title Page

Abstract

Introduction

Conclusions

References

Tables

Figures



Back

Close

Full Screen / Esc

Printer-friendly Version

Interactive Discussion



minor axis for each faecal pellet were performed with the Fiji software. The total number of spherical, ovoid, cylindrical, ellipsoid and tabular faecal pellets measured was 4041, 2047, 1338, 54 and 29, respectively. Using these dimensions, faecal pellet volume was determined using the appropriate shape equation (e.g. sphere, ellipse, cylinder, ovoid/ellipse) and converted to carbon using a factor of  $0.036 \text{ mg C mm}^{-3}$  (Gonzalez and Smetacek, 1994). Due to the irregularity of the tabular shapes preventing the use of single equation to calculate their volume, a constant value of  $119 \mu\text{g C pellet}^{-1}$  representing a midrange value for tabular shapes (Madin, 1982), was applied to tabular faecal pellets (Wilson et al., 2013). This value was relevant because the observed tabular faecal pellets were comprised in the size range reported in Madin (1982). Ranges and mean values of faecal pellet volumes and carbon content are reported in Table 3. Faecal fluff and disaggregated faecal pellets were not considered in these calculations because quantitative determination of their volume is difficult. We acknowledge that fragmentation of larger pellets may represent an artifact of the sample splitting procedure. Alternatively, their presence may also result from natural processes within the water column, although dedicated sampling techniques (e.g. polyacrylamide gel traps) are required to make this distinction (Ebersbach and Trull, 2008; Ebersbach et al., 2011, 2014; Laurenceau et al., 2014). Consequently our present quantification of faecal pellet carbon flux should be considered as lower-end estimates.

The precision of our calculations depends on the reliability of carbon-volume conversion factors of faecal pellets, which vary widely in the literature, as well as variability in diatom resting spore volumes (Table 2). To constrain the importance of this variability on our quantitative estimation of C flux, we calculated upper and lower error bounds by a constant scaling of the conversion factors ( $\pm 50\%$ ).

## 2.5 Statistical analyses

Correspondence analysis was performed to summarize the seasonality of diatom export assemblages. This approach projects the original variables (here full and empty cells) onto a few principal axes that concentrate the information of the Chi-squared



during the two intense events ( $2.60 \pm 0.03$  and  $2.19 \pm 0.10 \text{ mmol m}^{-2} \text{ d}^{-1}$ , mean  $\pm$  SD). LSi fluxes were highest in in spring ( $> 10 \mu\text{mol m}^{-2} \text{ d}^{-1}$  in cups #1 to #4, Table 1). The contribution of LSi to total particulate Si was 5 and 10 % respectively in cups #1 and #12 and lower than 3 % the remainder of the year. The POC : PON molar ratio showed low variability, ranging between 6 and 8.1, with a maximum value observed in autumn (cup #11). The BSi : POC molar ratio was highest at the beginning of the season (between  $2.18 \pm 0.19$  and  $3.46 \pm 0.16$  in the first three cups, blue line in Fig. 1c) and dropped to  $0.64 \pm 0.06$  in cup #5, following the first export event. BSi : POC ratios were close in the two export events ( $1.62 \pm 0.05$  and  $1.49 \pm 0.08$ ). The lowest BSi : POC ratio was observed in autumn in cup #11 ( $0.29 \pm 0.01$ ).

### 3.2 Diatom fluxes

Diatoms from 33 taxa were identified and their fluxes determined across the 11 months time series (Table 4). Full and empty cell fluxes for the total community and for the taxa that are the major contributors to total diatom flux (eight taxa that account for  $> 1$  % of total cells annual export) are presented in Fig. 2. The flux of full- and empty-cell fluxes for each diatom species or taxa is reported in Table 4.

During spring (cups #1 to #3) and winter (cups #11 and #12) the total flux of full cells was  $< 5 \times 10^6 \text{ cells m}^{-2} \text{ d}^{-1}$  (Fig. 2a). The total flux of full cells increased to  $5.5$  and  $9.5 \times 10^7 \text{ cells m}^{-2} \text{ d}^{-1}$  (cups #4 and #9, respectively) during two episodic ( $< 14$  days) sedimentation events. The two largest flux events (cups #4 and #9) were also associated with significant export of empty cells with respectively  $6.1 \times 10^7$  and  $2.9 \times 10^7 \text{ cells m}^{-2} \text{ d}^{-1}$  (Fig. 2a). For *Chaetoceros Hyalochaete* spp. resting spores (CRS), full cells fluxes of  $4 \times 10^7 \text{ cells m}^{-2} \text{ d}^{-1}$  and  $7.8 \times 10^7 \text{ cells m}^{-2} \text{ d}^{-1}$  accounted for 76 and 83 % of the total full cell flux during these two events, respectively (Fig. 2b), whereas a smaller contribution of *Thalassiosira antarctica* resting spores (TRS) ( $2.7 \times 10^6 \text{ cells m}^{-2} \text{ d}^{-1}$ , 5 % of total full cells) was observed during the first event (Fig. 2h). CRS also dominated (79–94 %) the composition of full cells in the interven-

## Export fluxes in a naturally fertilized area – Part 2

M. Rembauville et al.

Title Page

Abstract

Introduction

Conclusions

References

Tables

Figures



Back

Close

Full Screen / Esc

Printer-friendly Version

Interactive Discussion





## Export fluxes in a naturally fertilized area – Part 2

M. Rembauville et al.

Title Page

Abstract

Introduction

Conclusions

References

Tables

Figures



Back

Close

Full Screen / Esc

Printer-friendly Version

Interactive Discussion



on frequency distribution, therefore the results of the analysis must be considered as representative of the community composition as opposed to cell flux. The first two factors accounted for the majority (75.6 %) of total explained variance. Early in the season (cups #1–#3), during the period of biomass accumulation in the surface (Fig. 1a), diatom fluxes were characterized by empty cells of *T. nitzschioides* spp. and *F. kerguelensis*. Full TRS cells were observed in cup #3 following the initial bloom decline. The first major flux event (cup #4) contained mostly TRS, empty Small centrics (< 20 µm) cells and empty *C. Hyalochaete* spp. cells. The summer flux period (cups #5 to #8) primarily consisted of CRS, although *E. antarctica* var. *antarctica*, *Pseudo-nitzschia* spp. and *Thalassiothrix antarctica* were present as full cells and *Plagiotropis* spp., *Membraneis* spp., *Pseudo-nitzschia* spp. as empty cells. The second major flux event (cup #9) was tightly associated with CRS and full *Pseudo-nitzschia* spp. cells. Subsequent cups (#10 and #11) were characterized by full cells of *E. antarctica* var. *antarctica* and *Thalassiothrix antarctica* and empty cells of *Corethron inerme*, *P. alata*, *F. separanda/rhombica* and *F. kerguelensis*. Winter fluxes (cup #12) were similar to the initial three cups characterized primarily by empty cells of small diatom taxa. The centralized projection in Fig. 3 of full *F. kerguelensis* and *T. nitzschioides* spp. highlights their constant presence throughout the annual record.

The total empty : full cell ratio is presented in Fig. 2a (blue line). This ratio was highest in spring and early summer (cups #1 to #4), ranging between 1.1 and 2.4, suggesting more empty cells to full cells. The ratio was lowest, representing considerably more full cells to empty cells in cups #5 to #10 with values between 0.1 and 0.4. In autumn (cup #11), the empty : full ratio increased to 0.7. In the winter cup #12, the total amount of full diatom cells was very low and therefore we could not calculate a robust empty : full ratio. Across the time-series certain diatom taxa were observed exclusively as empty cells, notably *Chaetoceros atlanticus* f. *bulbosum*, and *Corethron pennatum*. For diatom taxa present as full and empty cells we calculated an annually integrated empty : full ratio (Fig. 4) and arbitrarily defined threshold values of 2 (representing species mainly observed as empty cells) and 0.5 (representing species mainly observed as full cells),

respectively. In decreasing order, the diatom taxa exhibiting empty : full ratios  $> 2$  were *Thalassiosira lentiginosa*, Small centrics ( $< 20 \mu\text{m}$ ), *Proboscia alata*, *Rhizosolenia antennata/styliformis*, *Chaetoceros decipiens*, *Corethron inerme*, *Dactyliosolen antarcticus*, Large centrics ( $> 20 \mu\text{m}$ ), and *Asteromphalus* spp. The diatom taxa displaying an empty : full ratio  $< 0.5$  were *Thalassiothrix antarctica*, *Rhizosolenia simplex*, CRS, *Eucampia antarctica* var. *antarctica*, *Thalassiosira* spp. and *Navicula* spp. Species or grouped taxa with ratio values falling between the thresholds ( $< 2$  and  $> 0.5$ ; *R. chunii*, through to *C. dichæta* in Fig. 4) were perceived as being almost equally represented by full and empty cells when integrated annually across the time series.

### 3.3 Faecal pellet fluxes

The seasonal flux of faecal pellet type, volume and their estimated carbon flux are summarized in Fig. 5 and Table 5. Total faecal pellet flux was  $< 2 \times 10^3$  pellets  $\text{m}^{-2} \text{d}^{-1}$  in spring (cups #1 to #3). Cups #4 and #5 were characterized by the highest fluxes of  $21.8 \times 10^3$  and  $5.1 \times 10^3$  pellets  $\text{m}^{-2} \text{d}^{-1}$  (Fig. 5a, Table 5). Faecal pellet numerical flux decreased gradually from mid-summer (cup# 5) to reach a minimal value in winter ( $140$  pellets  $\text{m}^{-2} \text{d}^{-1}$  in cup #12). In spring (cups #1 to #3), spherical and cylindrical shapes dominated the numerical faecal pellet fluxes. Ellipsoid and tabular shapes were absent from these spring cups. The first export event (cup #4), was numerically dominated by the spherical shaped pellets, however the remainder of the summer (cups #5 to #10) contained spherical, ovoid and cylindrical shapes in comparable proportions. Ellipsoid shapes were observed from mid-summer to autumn (cups #7 to #11) but their overall contribution to pellet flux was low ( $< 6\%$ , Table 5). Rare tabular shapes were observed in summer (cups #6 and #8) and their contribution to numerical fluxes was highest in autumn and winter (cups #11 and #12).

The median faecal pellet volume showed a seasonal signal with a maximum peak  $> 5.5 \times 10^6 \mu\text{m}^3$  in mid-summer (cups # 6 to #8) and values  $< 4 \times 10^6 \mu\text{m}^3$  the remainder of the year (Fig. 5b). Concomitantly with the highest median volume, the largest variance

BGD

11, 17089–17150, 2014

## Export fluxes in a naturally fertilized area – Part 2

M. Rembauville et al.

Title Page

Abstract

Introduction

Conclusions

References

Tables

Figures

◀

▶

◀

▶

Back

Close

Full Screen / Esc

Printer-friendly Version

Interactive Discussion



in faecal pellet size was also observed in the summer (highest interquartile values in Fig. 5b).

Total faecal pellet carbon flux was lowest in spring ( $< 0.05 \text{ mmol C m}^{-2} \text{ d}^{-1}$  in cups #1 to #3, Fig. 5c, Table 5). The highest total faecal pellet carbon flux of nearly  $0.5 \text{ mmol C m}^{-2} \text{ d}^{-1}$  was observed during the first export event in cup #4 and was essentially composed of spherical shapes (83 %, Table 5). For the remainder of the summer (cups #5 to #10), total faecal pellet carbon flux was between 0.03 and  $0.15 \text{ mmol C m}^{-2} \text{ d}^{-1}$  with a dominant contribution of cylindrical, ellipsoid and tabular shapes. In autumn and winter (cups #11 and #12), faecal pellet carbon fluxes of 0.13 and  $0.06 \text{ mmol C m}^{-2} \text{ d}^{-1}$  were strictly dominated by tabular shapes ( $> 90\%$  to total faecal pellet carbon fluxes, Table 5).

### 3.4 Statistical analysis of biological and biogeochemical signatures

The  $\beta$  correlation coefficients of standardized variables obtained from the PLSR analysis are presented as a heatmap in Fig. 6. The full cell fluxes of all diatom taxa, in addition to spherical and ovoid and ellipsoid faecal pellet fluxes were positively correlated to POC and PON fluxes. By contrast, empty cell fluxes of *F. kerguelensis*, *P. alata*, *T. nitzschioides* spp., *T. lentiginosa* and cylindrical, ellipsoid and tabular pellet fluxes were either uncorrelated or negatively correlated with POC and PON fluxes. Full- and empty-cell fluxes of all diatom taxa were positively correlated with BSi fluxes, although this correlation was notably weak for empty cells of *C. inerme*, *P. alata* and *T. lentiginosa*. Only spherical and ovoid faecal pellets were positively correlated with BSi fluxes. Full cells fluxes of CRS and *E. antarctica* var. *antarctica* were the most negatively correlated with BSi : POC molar ratio, whereas TRS, *F. kerguelensis*, *T. nitzschioides* spp. and *T. lentiginosa* full cells fluxes were positively correlated. Spherical and ovoid faecal pellets were weakly and negatively correlated with the BSi : POC molar ratio whereas the cylindrical, ellipsoid and tabular shapes were more strongly negatively correlated to the BSi : POC molar ratio. All the biological components exhibited weak or no correlations to the POC : PON molar ratio.

The first two latent vectors of the PLSR accounted for 61.3 and 74.1% of cumulative variance in  $X$  (full and empty diatom and pellet fluxes) and  $Y$  (biogeochemical properties). In order to visualize how the seasonal succession of flux vectors was related to the bulk geochemical properties of particles, the sampling cups, biological and chemical factors were projected on the first two latent factors of the PLSR analysis (Fig. 8). Positively projected on the first axis are the POC, PON and BSi fluxes, close to the export events sampled in cups #4 and #9. The closest biological components comprise a complex assemblage of full and empty cells and spherical and ovoid faecal pellet shapes. All the other cups are projected far from these two export events. The second axis opposes the spring cups (#1 to #3) to the autumn (#11) and winter (#12) cups. Empty frustules of *F. kerguelensis*, *T. lentiginosa* and *T. nitzschioides* spp. are projected close to the spring cups (#1 to #3) together with the BSi:POC molar ratio whereas autumn (#11) and winter cups (#12) are projected far from the BSi:POC molar ratio and close to the tabular and cylindrical faecal pellet shapes.

### 3.5 Partitioning carbon fluxes among ecological vectors

We estimated the contribution of resting spores and faecal pellets to carbon flux, calculated their cumulative values and compared them to measured values (Fig. 8a and b). A highly significant correlation (Spearman rank correlation,  $n = 36$ ,  $\rho = 0.84$ ,  $p < 0.001$ ) was evident between calculated and measured carbon flux suggesting that the main ecological flux vectors observed in the sample were capable of explaining the seasonal variation in total POC flux. Table 6 lists the contribution of each vector to the calculated flux. In cup #1, CRS and other diatoms dominated the calculated POC fluxes, with respectively 25.3 and 38.6%. Diatoms other than spores dominated the calculated carbon flux (35.4%) together with cylindrical faecal pellets (36.4%) in cup #2. TRS dominated the POC fluxes in cup #3 (85.1%). CRS strictly dominated the calculated POC fluxes in summer (cups #4 to #10) with a contribution ranging from 46.8 to 88.1%. During the autumn and winter (cups #11 and #12), POC fluxes were almost exclusively associated to tabular faecal pellets, 81 and 93.3%, respectively. At annual scale di-

atoms resting spores (CRS and TRS), other diatoms and faecal pellets respectively accounted for 60.7, 5 and 34.3% of the calculated POC fluxes. Annual POC fluxes estimated from ecological vectors considered here were slightly less than measured values (93.1 vs. 98.2 mmol m<sup>-2</sup>).

## 4 Discussion

### 4.1 The significance of resting spores for POC flux

Although there was generally a strong attenuation of flux between the base of the winter mixed layer (WML) and 300 m on the Kerguelen Plateau (Rembauville et al., 2014), we observed significant variability in export over the annual cycle. Generally POC fluxes were < 0.5 mmol m<sup>-2</sup> d<sup>-1</sup> with the notable exception of two pulsed (< 14 days) export events of ~ 1.5 mmol m<sup>-2</sup> d<sup>-1</sup> that accounted for ~ 40% of annual POC export. These two flux events were characterized by a noticeable increase and general dominance of diatom resting spores. During both of these pulsed export events, cumulative *Chaetoceros Hyalochaete* spp. resting spores (CRS) and *Thalassiosira antarctica* resting spores (TRS) fluxes accounted for 66 and 88% of the measured POC flux, whereas total faecal pellet flux accounted for 29 and 5.2%, respectively (Table 6). The combination of CRS and TRS were responsible for 60.7% of the annual calculated POC flux, a value ten times higher than the contribution of other diatoms (5%). We did not observe any full cells of the vegetative stage of *Chaetoceros Hyalochaete*, a feature possibly related to its high susceptibility to grazing pressure in the mixed layer (Smetacek et al., 2004; Quéguiner, 2013; Assmy et al., 2013). Empty *Chaetoceros Hyalochaete* spp. cells were vegetative stages different in shape from the resting spores. It can be the remaining of the vegetative stage after the spore formation or the result of the consumption of the organic material by grazing. Our flux data reveal that small (10 to 30 µm) and highly silicified resting spores bypass the intense grazing pressure char-

## Export fluxes in a naturally fertilized area – Part 2

M. Rembauville et al.

Title Page

Abstract

Introduction

Conclusions

References

Tables

Figures



Back

Close

Full Screen / Esc

Printer-friendly Version

Interactive Discussion



acterizing the base of the mixed layer, and are the primary mechanism through which carbon and, to a lesser extent silicon, is exported from the surface.

Numerous sediment trap studies have reported a strong contribution, if not dominance, of CRS to diatom fluxes at depth in various oceanographic regions (e.g. Antarctic Peninsula (Leventer, 1991), Bransfield Strait (Abelmann and Gersonde, 1991), Gulf of California (Sancetta, 1995; Lange, 1997), Eastern Equatorial Atlantic (Treppke et al., 1996), East China Sea (Kato et al., 2003), coastal North Pacific Ocean (Chang et al., 2013) and the subarctic Atlantic (Rynearson et al., 2013)). CRS are also found to be dominant in surface sediments in the coastal northeastern Pacific (Grimm et al., 1996), the North Atlantic (Bao et al., 2000), the northeast Pacific (Lopes et al., 2006), the North Scotia Sea (Allen et al., 2005), Antarctic sea ice and coastal regions (Crosta et al., 1997; Zielinski and Gersonde, 1997; Armand et al., 2005), and east of Kerguelen Island (Armand et al., 2008b). Moreover, the annual POC export from the A3 station sediment trap at 289 m ( $98.2 \pm 4.4 \text{ mmol m}^{-2} \text{ yr}^{-1}$ ) falls near annual estimates from deep sediment traps ( $> 2000 \text{ m}$ ) located in the naturally fertilized area downstream of the Crozet Islands ( $37\text{--}60$  and  $40\text{--}42 \text{ mmol m}^{-2} \text{ yr}^{-1}$ , Salter et al., 2012) where fluxes were considered as mainly driven by resting spores of *Eucampia antarctica* var. *antarctica*. The frequent occurrence and widespread distribution of diatoms resting spores suggest their pivotal role in the efficient transfer of carbon to depth. Although they are frequently observed in blooms heavily influenced by the proximity of the coast, large-scale advection might explain that their impact on carbon export is not restricted to neritic areas.

*Chaetoceros* resting spores have been reported to contain up to 10 times more carbon than the vegetative forms (Kuwata et al., 1993) with no vacuole and high contents of lipids and carbohydrates (Doucette and Fryxell, 1983; Kuwata et al., 1993). Moreover, CRS resist grazing and have been found to lower copepods grazing pressure (Kuwata and Tsuda, 2005). We suggest that diatom resting spores gather three essential characteristics for intense POC export to the deep ocean: (1) they efficiently bypass the grazing pressure near the mixed layer due to their morphological char-

## BGD

11, 17089–17150, 2014

### Export fluxes in a naturally fertilized area – Part 2

M. Rembauville et al.

Title Page

Abstract

Introduction

Conclusions

References

Tables

Figures



Back

Close

Full Screen / Esc

Printer-friendly Version

Interactive Discussion



## Export fluxes in a naturally fertilized area – Part 2

M. Rembauville et al.

Title Page

Abstract

Introduction

Conclusions

References

Tables

Figures



Back

Close

Full Screen / Esc

Printer-friendly Version

Interactive Discussion



acteristics such as very robust frustules (CRS) or numerous spines (TRS) (high export efficiency), (2) they are efficiently transferred to depth due to the thick and dense frustule increasing sinking velocity and (3) their high carbon content is protected from microbial degradation by the thick frustules (these last two points result in a high transfer efficiency). The spatial distribution and formation of resting spores may therefore be an integral ecological component defining the strength and efficiency of the biological pump. Nutrient depletion has been shown to trigger resting spore formation in *Chaetoceros Hyalochaete* laboratory cultures (Garrison, 1981; Sanders and Cibik, 1985; Kuwata et al., 1993; Oku and Kamatani, 1997) over relatively rapid timescales (6 to 48 h, McQuoid and Hobson, 1996). Although  $\text{Si}(\text{OH})_4$  depletion appears to be the most likely biogeochemical trigger at the Kerguelen Plateau (from  $24 \mu\text{mol L}^{-1}$  in early spring to  $2 \mu\text{mol L}^{-1}$  in summer, Mosseri et al., 2008; Closset et al., 2014), other environmental factors (iron or light availability) could influence the resting spore formation. Further work to establish seasonal dynamics of these factors linked to diatom life cycle and specifically the resting spore formation response is necessary.

### 4.2 Contribution of faecal pellets to POC flux

Although diatoms resting spores are the primary vector for POC flux below the mixed layer, faecal pellets were also important and accounted for 34.3% of annual export. It could be hypothesized that faecal pellets are the dominant flux component in High Biomass, Low Export (HBLE) environments, where biomass is routed to higher trophic levels (Lam and Bishop, 2007; Ebersbach et al., 2011). However, this hypothesis does not appear to be true for the bloom of the central Kerguelen Plateau suggesting that faecal material is efficiently reprocessed in the mixed layer, or that a significant part of the pellet flux is excreted below the trap depth by vertically migrating zooplankton. Small spherical faecal pellets dominated the annual numerical faecal pellet flux (53.8%, Table 5). The short and intense export of small spherical faecal pellet was concomitant with the first strong POC export in cup #4 (Table 5). The significance of small spherical faecal pellets to POC flux is somewhat uncharacteristic in comparison

to other sediment trap records in shallow areas of the Southern Ocean (Schnack-Schiel and Isla, 2005). They are possibly produced by small cyclopoid copepods, like *Oithona similis* that are abundant in the POOZ (Fransz and Gonzalez, 1995; Pinkerton et al., 2010). More specifically, *O. similis* represents > 50 % of mesozooplankton abundance at A3 in spring (Carlotti et al., 2014) and have been observed at station A3 in summer (Carlotti et al., 2008). *Oithona* species are known to be coprophagous and play an important role in flux reprocessing (Gonzalez and Smetacek, 1994), which may partially contribute to the rapid flux attenuation observed by efficiently retaining carbon in the mixed layer. This reprocessing feeding strategy might also explain the low faecal pellet flux we observed (highest value of  $21.8 \times 10^3 \text{ pellet m}^{-2} \text{ d}^{-1}$ ), which was two orders of magnitude lower than the  $> 5 \times 10^5 \text{ pellet m}^{-2} \text{ d}^{-1}$  observed in neritic areas where euphausiids dominate the mesozooplankton community (Bodungen, 1986; von Bodungen et al., 1987; Wefer et al., 1988).

There are notable differences in faecal pellet type over the course of the season. The transition from spherical and ovoid pellets in spring to larger cylindrical and tabular pellets in summer presumably reflects shifts in dominant zooplankton species from small cyclopoid copepods towards larger calanoid copepods, euphausiids and salps (e.g. Wilson et al., 2013). Carlotti et al. (2014) report that mesozooplankton biomass doubled between October and November 2011 and was three fold higher in January 2005 (Carlotti et al., 2008). In spring, Carlotti et al. (2014) observed that the small size fraction (300–500  $\mu\text{m}$ ) was numerically dominated by *Oithona similis* (50% of the total mesozooplankton assemblage), although the larger size fractions dominated the mesozooplankton biomass (dominated by *Clausocalanus citer*, and *Rhicalanus gigas*). This is consistent with the dominance of small spherical faecal pellets and the lower contribution of cylindrical shapes we observed in spring and early summer (cups #1 to #4, Table 4). In summer (January 2005), the mesozooplankton community was more diversified and comprised 21 % of small individuals (*Oithona* sp. and *Oncea* sp.), 20 % of medium-sized individuals (*Clausocalanus* sp. and *Microcalanus* sp.) and 21 % of large individuals (*Calanus* sp., *Metrida* sp., *Paraeuchaeta* sp., *Pleuromama* sp. and *Rhin-*

## BGD

11, 17089–17150, 2014

### Export fluxes in a naturally fertilized area – Part 2

M. Rembauville et al.

Title Page

Abstract

Introduction

Conclusions

References

Tables

Figures



Back

Close

Full Screen / Esc

Printer-friendly Version

Interactive Discussion



## Export fluxes in a naturally fertilized area – Part 2

M. Rembauville et al.

Title Page

Abstract

Introduction

Conclusions

References

Tables

Figures



Back

Close

Full Screen / Esc

Printer-friendly Version

Interactive Discussion



*calanus* sp.; Carlotti et al., 2008). As the median size of faecal pellets increases, so does their relative contribution to carbon flux (Fig. 5b and d, Table 5). Our observation of an increasing contribution of cylindrical faecal pellet shapes in summer (cups #5 to #10, Table 5) is consistent with the increasing contribution of large calanoid copepods to the mesozooplankton assemblages. We note that pteropods showed the highest contribution to mesozooplankton assemblages at station A3 in summer (16% of total abundance, Carlotti et al., 2008). We associate this observation with the large ellipsoid faecal pellet shape that was first observed in the sediment trap in cup #5 (end December 2011) and represented the highest contribution to faecal pellet carbon fluxes in cup #9 (January/February 2012, Table 5). Tabular faecal pellets dominate the low POC fluxes observed in the autumn and winter when chlorophyll *a* concentration was reduced to background levels, although this interpretation should be taken with caution since a constant and high carbon content was used for this shape. The increase in organic carbon content and negative correlation between the abundance of cylindrical, ellipsoid and tabular faecal pellets fluxes and the BSi : POC molar ratio suggests that large zooplankton producing these tabular pellets (large copepods, euphausiids and salps) are not feeding directly on diatoms. During the autumn and winter, microbial components other than diatoms must sustain the production of this large zooplankton. Direct observation of faecal pellet content is beyond the scope of the present study but would help to elucidate how seasonal trends of zooplankton feeding ecology influence carbon and biomineral export. Moreover, dedicated studies are still needed to document the seasonal dynamic of euphausiids and salps abundances over the Kerguelen Plateau to compare them with our reported faecal pellet fluxes.

### 4.3 Diatom fluxes

The diatom fluxes (sum of empty and full cells) observed at the central Kerguelen Plateau reached their maximum value of  $1.2 \times 10^8 \text{ cells m}^{-2} \text{ d}^{-1}$  during the two short export events. This value falls between the POOZ ( $\sim 10^7 \text{ cells m}^{-2} \text{ d}^{-1}$ , Abellmann and Gersonde, 1991; Salter et al., 2012; Grigorov et al., 2014) and the SIZ

( $> 10^9$  cells  $m^{-2} d^{-1}$ , Suzuki et al., 2001; PilskaIn et al., 2004). The values are similar to the  $2.5\text{--}3.5 \times 10^8$  cell  $m^{-2} d^{-1}$  measured at 200 m in a coastal station of the Antarctic Peninsula, where CRS represented  $\sim 80\%$  of the phytoplankton assemblage (Leventer, 1991). Although the resting spore formation strategy is typically associated with neritic areas (Smetacek, 1985; Crosta et al., 1997; Salter et al., 2012), their very high export and transfer efficiency together with advection can explain their contribution to deep open ocean fluxes (e.g. Rynearson et al., 2013).

During a previous multidisciplinary process study of the Kerguelen Plateau (KEOPS1, 2005), a shift in plankton community composition was observed at station A3 between January and February. The surface community initially dominated by *Chaetoceros Hyalochaete* vegetative chains gave way to one dominated by *Eucampia antarctica* var. *antarctica*, concomitant with increasing CRS abundance in the mixed layer (Armand et al., 2008a). The abundance of dead cells (within chains or as empty single cells and half cells) in the surface water column also increased from January to February, suggesting intense heterotrophic activity. Surface sediments at station A3 contain, in decreasing abundance, *F. kerguelensis*, CRS and *T. nitzschioides* spp. cells (Armand et al., 2008b). These sedimentary distributions are consistent with the dominant species observed in the sediment trap, *F. kerguelensis* and *T. nitzschioides* spp. being present throughout the year and mostly represented by empty cells whereas CRS are exported during short and intense events.

*Eucampia antarctica* var. *antarctica* resting spores dominated the deep (2000 m) sediment trap diatom assemblages in the naturally fertilized area close to the Crozet Islands with fluxes  $> 10^7$  cells  $m^{-2} d^{-1}$  (Salter et al., 2012). We observed highest *Eucampia antarctica* var. *antarctica* full cells fluxes of  $\sim 10^6$  cells  $m^{-2} d^{-1}$  in summer, which represents  $< 10\%$  of the total cell flux. Both vegetative and resting stages were observed. Our results suggest that *Eucampia antarctica* var. *antarctica* is unlikely to be a major driving vector for carbon fluxes to depth over the central Kerguelen Plateau, in part because the community was not forming massive highly-silicified, fast-sinking resting spores contrary to observations near the Crozet Islands. Moreover their bio-

BDG

11, 17089–17150, 2014

## Export fluxes in a naturally fertilized area – Part 2

M. Rembauville et al.

Title Page

Abstract

Introduction

Conclusions

References

Tables

Figures



Back

Close

Full Screen / Esc

Printer-friendly Version

Interactive Discussion







et al., 2006). However, the ten-fold differences in BSi : POC ratios of exported particles between spring and summer is unlikely to result simply from physiological constraints set during diatoms growth (Hutchins and Bruland, 1998; Takeda, 1998). Previous comparisons in natural and artificially iron-fertilized settings have the highlighted importance of diatom community structure for carbon and silica export (Smetacek et al., 2004; Salter et al., 2012; Quéguiner, 2013; Assmy et al., 2013). The presence of different diatom species and their characteristic traits (e. g. susceptibility to grazing, apoptosis, viral lysis) are all likely to influence the flux of full and empty cells. Therefore, the net BSi : POC export ratio results from the net effect of species specific Si:C composition (Sackett et al., 2014) and the subsequent species-specific mortality pathway and dissolution. A significant correlation between BSi : POC and empty : full cells ratio (Spearman rank correlation,  $n = 12$ ,  $\rho = 0.78$ ,  $p < 0.05$ ) suggests the latter acts as a first order control on the silicon and organic carbon export stoichiometry.

We classified species that were observed exclusively as empty cells, or sinking with an integrated empty : full ratio  $> 2$ , as predominantly silica exporters and these included: *C. bulbosum*, *C. pennatum*, *P. truncata*, *R. antennata/styliformis*, *A. hookeri*, *A. hyalinus*, *C. decipiens*, *C. inerme*, *D. antarcticus*, *P. alata*, *T. nitzschioides* spp., *T. lentiginosa*, and small centric species ( $< 20 \mu\text{m}$ ). Although *F. kerguelensis*, *T. nitzschioides* spp. and *T. lentiginosa* were present through the entire season, their fluxes were highly correlated with BSi : POC ratios (Fig. 6) identifying these species as significant contributors to silica export. On the contrary resting spores and species that sink with a major contribution of full cells (integrated empty-full ratio  $< 0.5$ ) were identified as belonging to the preferential carbon sinkers: *C. Hyalochaete* spp., *E. antarctica* var. *antarctica*, *R. simplex* and *Thalassiothrix antarctica*. Among them, CRS and *E. antarctica* var. *antarctica* were the most negatively correlated to the BSi : POC ratio and were identified as key species for carbon export (Fig. 6). These observations are consistent with previous studies of natural (Salter et al., 2012) and artificial (Assmy et al., 2013) iron fertilization that identified *C. pennatum*, *D. antarcticus* and *F. kerguelensis* as major silica sinkers and *C. Hyalochaete* vegetative cells, CRS and *E. antarctica* var. *antarctica*

## Export fluxes in a naturally fertilized area – Part 2

M. Rembauville et al.

[Title Page](#)[Abstract](#)[Introduction](#)[Conclusions](#)[References](#)[Tables](#)[Figures](#)[Back](#)[Close](#)[Full Screen / Esc](#)[Printer-friendly Version](#)[Interactive Discussion](#)

resting spores as major carbon sinkers. Notably, resting spore formation was not observed in the artificial experiment and carbon export was attributed to mass mortality and aggregation of algal cells (Assmy et al., 2013). Nevertheless, a more detailed analysis of species-specific carbon and silica content in the exported material is necessary to fully validate their respective role on carbon and silica export.

#### 4.5 Seasonal succession of ecological flux vectors over the Kerguelen Plateau

Although sediment trap records integrate cumulative processes of production in the mixed layer and losses during export, they provide a unique insight into the temporal succession of plankton functional types and resultant geochemical properties of exported particles characterizing the biological pump. The robustness of the relationship between measured and calculated POC fluxes suggests that the main ecological flux vectors described from our sediment trap samples are sufficient to model the seasonal evolution of total POC fluxes (Fig. 8b). At an annual scale the calculated POC fluxes slightly underestimate those measured (93.1 vs. 98.2 mmol m<sup>-2</sup>), which might result from the minor contribution of full cells other than the diatoms species considered, in addition to aggregated material, organic matter sorbed to the exterior of empty cells and faecal fluff that was difficult to enumerate. In spring, carbon fluxes are low and mainly associated with the empty cells of small diatoms and small faecal pellets. In summer carbon fluxes are primarily driven by resting spores, whereas the contribution of small faecal pellets is low. In winter, when primary production is negligible, large faecal pellets become the major carbon flux vector.

The species succession directly observed in our sediment trap samples differs somewhat to the conceptual model of ecological succession in naturally iron fertilized areas proposed by Quéguiner (2013), although the general patterns are similar. The first diatoms exported in spring are indeed small species of *F. kerguelensis*, *T. nitzschoides* spp., and small centric species (< 20 μm). However we observe that these species are exported almost exclusively as empty cells. The abundance of small spherical and ovoid faecal pellet suggests an important role of small copepods in the zooplankton

### Export fluxes in a naturally fertilized area – Part 2

M. Rembauville et al.

Title Page

Abstract

Introduction

Conclusions

References

Tables

Figures



Back

Close

Full Screen / Esc

Printer-friendly Version

Interactive Discussion



(Yoon et al., 2001; Wilson et al., 2013), which was corroborated by the finding of dominant *Oithona similis* abundances in the spring mesozooplankton assemblages at station A3 (Carlotti et al., 2014). Therefore, our data suggests that spring export captured by the sediment trap was the remnants of a diatom community subject to efficient grazing and carbon utilization in, or at the basis of, the mixed layer, resulting in a BSi : POC export ratio > 2 (Table 1).

The main difference in our observations and the conceptual scheme of Quéguiner (2013) is the dominance of *Chaetoceros Hyalochaete* resting spores to diatom export assemblages and their contribution to carbon fluxes out of the mixed layer in summer, probably triggered by  $\text{Si(OH)}_4$  limitation. Resting spores appear to efficiently bypass the “carbon trap” represented by grazers and might also physically entrain small faecal pellets in their downward flux. In mid-summer, faecal pellet carbon export is dominated by the contribution of cylindrical shapes. This appears to be consistent with an observed shift toward a higher contribution of large copepods and euphausiids to the mesozooplankton community in the mixed layer (Carlotti et al., 2008). However, CRS still dominate the diatom exported assemblage. The corresponding BSi : POC ratio decreases with values between 1 and 2 (Table 1). The fact that there are two discrete resting sport export events might be explained by a mixing event that injected  $\text{Si(OH)}_4$  into the surface allowing the development of a secondary  $\text{Si(OH)}_4$  limitation.

In the autumn and winter, diatoms fluxes are very low and faecal pellet carbon export is dominated by cylindrical and tabular contributions consistent with a supposed shift to zooplankton communities dominated by large copepods, euphausiids, and salps (Wilson et al., 2013). The low BSi : POC ratios characterizing export at this time suggest that these communities feed primarily suspended particles (in the case of salps) and on micro- and mesozooplankton or small diatoms, although direct measurements of faecal pellet content would be necessary to confirm this.

## BGD

11, 17089–17150, 2014

### Export fluxes in a naturally fertilized area – Part 2

M. Rembauville et al.

Title Page

Abstract

Introduction

Conclusions

References

Tables

Figures



Back

Close

Full Screen / Esc

Printer-friendly Version

Interactive Discussion



## 5 Conclusions

We report the chemical (particulate organic carbon and nitrogen, biogenic silica) and biological (diatom cells and faecal pellets) composition of material exported beneath the winter mixed layer (289 m) in a naturally iron-fertilized area of the Southern Ocean. Despite iron availability, annually integrated organic carbon export was low (98 mmol m<sup>-2</sup>) although biogenic silicon export was significant (114 mmol m<sup>-2</sup>). *Chaetoceros Hyalochaete* and *Thalassiosira antarctica* resting spores accounted for more than 60 % of the annual POC flux. The high abundance of empty cells and the low contribution of faecal pellets to POC flux (34 %) suggest efficient carbon retention occurs in, or at the base of the mixed layer. We propose that in this HBLE environment, carbon-rich and fast sinking resting spores bypass the intense grazing pressure otherwise responsible for the rapid attenuation of flux. The seasonal succession of diatom taxa groups was tightly linked to the stoichiometry of the exported material. Several species were identified as primarily “silica sinkers” e.g. *Fragilariopsis kerguelensis* and *Thalassionema nitzschioides* spp. and others as preferential “carbon sinkers” e.g. resting spores of *Chaetoceros Hyalochaete* and *Thalassiosira antarctica*, *Eucampia antarctica* var. *antarctica* and the giant diatom *Thalassiothrix antarctica*. Faecal pellet types described a clear transition from small spherical shapes (small copepods) in spring, larger cylindrical and ellipsoid shapes in summer (euphausiids and large copepods) and large tabular shape (salps) in fall. Their contribution to carbon fluxes increased with the presence of larger shapes.

The change in biological productivity and ocean circulation cannot explain the ~ 80 ppmv atmospheric pCO<sub>2</sub> difference between the preindustrial era and the last glacial maximum (Archer et al., 2000; Bopp et al., 2003; Kohfeld et al., 2005; Wolff et al., 2006). Nevertheless, a simple switch in “silica sinker” vs. “carbon sinker” relative abundance would have a drastic effect on carbon sequestration in the Southern Ocean and silicic acid availability at lower latitudes (Sarmiento et al., 2004; Boyd, 2013). The results presented here emphasize the compelling need for similar studies in other locations

BGD

11, 17089–17150, 2014

### Export fluxes in a naturally fertilized area – Part 2

M. Rembauville et al.

Title Page

Abstract

Introduction

Conclusions

References

Tables

Figures



Back

Close

Full Screen / Esc

Printer-friendly Version

Interactive Discussion



of the global Ocean that will allow identification of key ecological vectors that set the magnitude and the stoichiometry of the biological pump.

*Acknowledgements.* We thank the Captain Bernard Lassiette and his crew during the KEOPS2 mission on the R/V *Marion Dufresne II*. We thank Karine Leblanc and Marine Lasbleiz for their constructive comments, which helped us to improve the manuscript. This work was supported by the French Research program of INSU-CNRS LEFE-CYBER (Les enveloppes fluides et l'environnement – Cycles biogéochimiques, environnement et ressources), the French ANR (Agence Nationale de la Recherche, SIMI-6 program, ANR-10-BLAN-0614), the French CNES (Centre National d'Etudes Spatiales) and the French Polar Institute IPEV (Institut Polaire Paul-Emile Victor). L. Armand's participation in the KEOPS2 program was supported by an Australian Antarctic Division grant (#3214).

## References

- Abdi, H.: Partial least squares regression and projection on latent structure regression (PLS Regression), *Wiley Interdiscip. Rev. Comput. Stat.*, 2, 97–106, doi:10.1002/wics.51, 2010.
- Abelmann, A. and Gersonde, R.: Biosiliceous particle flux in the Southern Ocean, *Biochemistry and circulation of water masses in the Southern Ocean International Symposium*, *Mar. Chem.*, 35, 503–536, doi:10.1016/S0304-4203(09)90040-8, 1991.
- Allen, C. S., Pike, J., Pudsey, C. J., and Leventer, A.: Submillennial variations in ocean conditions during deglaciation based on diatom assemblages from the southwest Atlantic, *Paleoceanography*, 20, PA2012, doi:10.1029/2004PA001055, 2005.
- Aminot, A. and Kerouel, R.: *Dosage automatique des nutriments dans les eaux marines: méthodes en flux continu*, Ifremer, Plouzané, France, 2007.
- Archer, D., Winguth, A., Lea, D., and Mahowald, N.: What caused the glacial/interglacial atmospheric  $p\text{CO}_2$  cycles?, *Rev. Geophys.*, 38, 159–189, doi:10.1029/1999RG000066, 2000.
- Armand, L. K., Cornet-Barthaux, V., Mosseri, J., and Quéguiner, B.: Late summer diatom biomass and community structure on and around the naturally iron-fertilised Kerguelen Plateau in the Southern Ocean, KEOPS: Kerguelen Ocean and Plateau compared Study, *Deep-Sea Res. Pt. II*, 55, 653–676, doi:10.1016/j.dsr2.2007.12.031, 2008a.

BGD

11, 17089–17150, 2014

## Export fluxes in a naturally fertilized area – Part 2

M. Rembauville et al.

Title Page

Abstract

Introduction

Conclusions

References

Tables

Figures



Back

Close

Full Screen / Esc

Printer-friendly Version

Interactive Discussion



## Export fluxes in a naturally fertilized area – Part 2

M. Rembauville et al.

Title Page

Abstract

Introduction

Conclusions

References

Tables

Figures



Back

Close

Full Screen / Esc

Printer-friendly Version

Interactive Discussion



Armand, L. K., Crosta, X., Quéguiner, B., Mosseri, J., and Garcia, N.: Diatoms preserved in surface sediments of the northeastern Kerguelen Plateau, *Deep-Sea Res. Pt. II*, 55, 677–692, doi:10.1016/j.dsr2.2007.12.032, 2008b.

Armand, L. K., Crosta, X., Romero, O., and Pichon, J.-J.: The biogeography of major diatom taxa in Southern Ocean sediments: 1. Sea ice related species, *Palaeogeogr. Palaeoclimatol.*, 223, 93–126, doi:10.1016/j.palaeo.2005.02.015, 2005.

Arrigo, K. R., Worthen, D., Schnell, A., and Lizotte, M. P.: Primary production in Southern Ocean waters, *J. Geophys. Res.-Oceans*, 103, 15587–15600, doi:10.1029/98JC00930, 1998.

Assmy, P., Smetacek, V., Montresor, M., Klaas, C., Henjes, J., Strass, V. H., Arrieta, J. M., Bathmann, U., Berg, G. M., Breitbarth, E., Cisewski, B., Friedrichs, L., Fuchs, N., Herndl, G. J., Jansen, S., Krägel, S., Latasa, M., Peeken, I., Röttgers, R., Scharek, R., Schüller, S. E., Steigenberger, S., Webb, A., and Wolf-Gladrow, D.: Thick-shelled, grazer-protected diatoms decouple ocean carbon and silicon cycles in the iron-limited Antarctic Circumpolar Current, *P. Natl. Acad. Sci. USA*, 110, 20633–20638, 2013.

Baker, E. T., Milburn, H. B., and Tennant, D. A.: Field assessment of sediment trap efficiency under varying flow conditions, *J. Mar. Res.*, 46, 573–592, doi:10.1357/002224088785113522, 1988.

Bao, R., Stigter, H. D., and Weering, T. C. E. V.: Diatom fluxes in surface sediments of the Goban Spur continental margin, NE Atlantic Ocean, *J. Micropalaeontol.*, 19, 123–131, doi:10.1144/jm.19.2.123, 2000.

Blain, S., Tréguer, P., Belviso, S., Bucciarelli, E., Denis, M., Desabre, S., Fiala, M., Martin Jézéquel, V., Le Fèvre, J., Mayzaud, P., Marty, J.-C., and Razouls, S.: A biogeochemical study of the island mass effect in the context of the iron hypothesis: Kerguelen Islands, Southern Ocean, *Deep-Sea Res. Pt. I*, 48, 163–187, doi:10.1016/S0967-0637(00)00047-9, 2001.

Blain, S., Quéguiner, B., Armand, L., Belviso, S., Bombled, B., Bopp, L., Bowie, A., Brunet, C., Brussaard, C., Carlotti, F., Christaki, U., Corbière, A., Durand, I., Ebersbach, F., Fuda, J.-L., Garcia, N., Gerringa, L., Griffiths, B., Guigue, C., Guillerm, C., Jacquet, S., Jandel, C., Laan, P., Lefèvre, D., Lo Monaco, C., Malits, A., Mosseri, J., Obernosterer, I., Park, Y.-H., Picheral, M., Pondaven, P., Remenyi, T., Sandroni, V., Sarthou, G., Savoye, N., Scouarnec, L., Souhaut, M., Thuiller, D., Timmermans, K., Trull, T., Uitz, J., van Beek, P., Veldhuis, M., Vincent, D., Viollier, E., Vong, L., and Wagener, T.: Effect of natural iron fertilization on carbon sequestration in the Southern Ocean, *Nature*, 446, 1070–1074, doi:10.1038/nature05700, 2007.

## Export fluxes in a naturally fertilized area – Part 2

M. Rembauville et al.

Title Page

Abstract

Introduction

Conclusions

References

Tables

Figures



Back

Close

Full Screen / Esc

Printer-friendly Version

Interactive Discussion



Blain, S., Renaut, S., Xing, X., Claustre, H., and Guinet, C.: Instrumented elephant seals reveal the seasonality in chlorophyll and light-mixing regime in the iron-fertilized Southern Ocean, *Geophys. Res. Lett.*, 40, 6368–6372, doi:10.1002/2013GL058065, 2013.

Bopp, L., Kohfeld, K. E., Le Quéré, C., and Aumont, O.: Dust impact on marine biota and atmospheric CO<sub>2</sub> during glacial periods, *Paleoceanography*, 18, 1046, doi:10.1029/2002PA000810, doi:10.1029/2002PA000810, 2003.

Boyd, P. W.: Diatom traits regulate Southern Ocean silica leakage, *P. Natl. Acad. Sci. USA*, 110, 20358–20359, doi:10.1073/pnas.1320327110, 2013.

Brzezinski, M. A.: The Si:C:N ratio of marine diatoms: interspecific variability and the effect of some environmental variables, *J. Phycol.*, 21, 347–357, doi:10.1111/j.0022-3646.1985.00347.x, 1985.

Brzezinski, M. A., Pride, C. J., Franck, V. M., Sigman, D. M., Sarmiento, J. L., Matsumoto, K., Gruber, N., Rau, G. H., and Coale, K. H.: A switch from Si(OH)<sub>4</sub> to NO<sub>3</sub><sup>-</sup> depletion in the glacial Southern Ocean, *Geophys. Res. Lett.*, 29, 1564, doi:10.1029/2001GL014349, 2002.

Buesseler, K. O.: The decoupling of production and particulate export in the surface ocean, *Global Biogeochem. Cy.*, 12, 297–310, doi:10.1029/97GB03366, 1998.

Buesseler, K. O., Steinberg, D. K., Michaels, A. F., Johnson, R. J., Andrews, J. E., Valdes, J. R., and Price, J. F.: A comparison of the quantity and composition of material caught in a neutrally buoyant vs. surface-tethered sediment trap, *Deep-Sea Res. Pt. I*, 47, 277–294, doi:10.1016/S0967-0637(99)00056-4, 2000.

Buesseler, K. O., Antia, A. N., Chen, M., Fowler, S. W., Gardner, W. D., Gustafsson, Ö., Harada, K., Michaels, A. F., Rutgers v. d. Loeff, M., Sarin, M., Steinberg, D. K., and Trull, T.: An assessment of the use of sediment traps for estimating upper ocean particle fluxes, *J. Mar. Res.*, 65, 345–416., 2007.

Burd, A. B. and Jackson, G. A.: Particle aggregation, *Annu. Rev. Mar. Sci.*, 1, 65–90, doi:10.1146/annurev.marine.010908.163904, 2009.

Carlotti, F., Thibault-Botha, D., Nowaczyk, A., and Lefèvre, D.: Zooplankton community structure, biomass and role in carbon fluxes during the second half of a phytoplankton bloom in the eastern sector of the Kerguelen Shelf (January–February 2005), *KEOPS: Kerguelen Ocean and Plateau compared Study*, *Deep-Sea Res. Pt. II*, 55, 720–733, doi:10.1016/j.dsr2.2007.12.010, 2008.

---

**Export fluxes in  
a naturally fertilized  
area – Part 2**M. Rembauville et al.

---

[Title Page](#)[Abstract](#)[Introduction](#)[Conclusions](#)[References](#)[Tables](#)[Figures](#)[Back](#)[Close](#)[Full Screen / Esc](#)[Printer-friendly Version](#)[Interactive Discussion](#)

Carlotti, F., Jouandet, M.-P., Nowaczyk, A., Harmelin-Vivien, M., Lefèvre, D., Guillou, G., Zhu, Y., and Zhou, M.: Mesozooplankton structure and functioning during the onset of the Kerguelen Bloom during KEOPS2 survey, Biogeosciences, in preparation, 2014.

Chang, A. S., Bertram, M. A., Ivanochko, T., Calvert, S. E., Dallimore, A., and Thomson, R. E.: Annual record of particle fluxes, geochemistry and diatoms in Effingham Inlet, British Columbia, Canada, and the impact of the 1999 La Niña event, Mar. Geol., 337, 20–34, doi:10.1016/j.margeo.2013.01.003, 2013.

Closset, I., Lasbleiz, M., Leblanc, K., Quéguiner, B., Cavagna, A.-J., Elskens, M., Navez, J., and Cardinal, D.: Seasonal evolution of net and regenerated silica production around a natural Fe-fertilized area in the Southern Ocean estimated with Si isotopic approaches, Biogeosciences, 11, 5827–5846, doi:10.5194/bg-11-5827-2014, 2014.

Cornet-Barthaux, V., Armand, L., and Quguiner, B.: Biovolume and biomass estimates of key diatoms in the Southern Ocean, Aquat. Microb. Ecol., 48, 295–308, doi:10.3354/ame048295, 2007.

Crawford, R.: The role of sex in the sedimentation of a marine diatom bloom, Limnol. Oceanogr., 40, 200–204., 1995.

Crosta, X., Pichon, J.-J., and Labracherie, M.: Distribution of Chaetoceros resting spores in modern peri-Antarctic sediments, Mar. Micropaleontol., 29, 283–299, doi:10.1016/S0377-8398(96)00033-3, 1997.

Davison, P. C., Checkley Jr., D. M., Koslow, J. A., and Barlow, J.: Carbon export mediated by mesopelagic fishes in the northeast Pacific Ocean, Prog. Oceanogr., 116, 14–30, doi:10.1016/j.pcean.2013.05.013, 2013.

DeMaster, D. J.: The supply and accumulation of silica in the marine environment, Geochim. Cosmochim. Ac., 45, 1715–1732, doi:10.1016/0016-7037(81)90006-5, 1981.

Doucette, G. J. and Fryxell, G. A.: Thalassiosira antarctica: vegetative and resting stage chemical composition of an ice-related marine diatom, Mar. Biol., 78, 1–6, doi:10.1007/BF00392964, 1983.

Dubischar, C. D. and Bathmann, U. V.: The occurrence of faecal material in relation to different pelagic systems in the Southern Ocean and its importance for vertical flux, the Southern Ocean II: climatic changes and the cycle of carbon, Deep-Sea Res. Pt. II, 49, 3229–3242, doi:10.1016/S0967-0645(02)00080-2, 2002.

Dunbar, R. B.: Sediment trap experiments on the Antarctic continental margin, Antarct. J. US, 19, 70–71, 1984.

## Export fluxes in a naturally fertilized area – Part 2

M. Rembauville et al.

Title Page

Abstract

Introduction

Conclusions

References

Tables

Figures



Back

Close

Full Screen / Esc

Printer-friendly Version

Interactive Discussion



Dutkiewicz, S., Follows, M. J., and Parekh, P.: Interactions of the iron and phosphorus cycles: a three-dimensional model study, *Global Biogeochem. Cy.*, 19, GB1021, doi:10.1029/2004GB002342, 2005.

Ebersbach, F. and Trull, T. W.: Sinking particle properties from polyacrylamide gels during the Kerguelen Ocean and Plateau compared Study (KEOPS): zooplankton control of carbon export in an area of persistent natural iron inputs in the Southern Ocean, *Limnol. Oceanogr.*, 53, 212–224, doi:10.4319/lo.2008.53.1.0212, 2008.

Ebersbach, F., Trull, T. W., Davies, D. M., and Bray, S. G.: Controls on mesopelagic particle fluxes in the Sub-Antarctic and Polar Frontal Zones in the Southern Ocean south of Australia in summer – perspectives from free-drifting sediment traps, *Deep-Sea Res. Pt. II*, 58, 2260–2276, doi:10.1016/j.dsr2.2011.05.025, 2011.

Ebersbach, F., Assmy, P., Martin, P., Schulz, I., Wolzenburg, S., and Nöthig, E.-M.: Particle flux characterisation and sedimentation patterns of protistan plankton during the iron fertilisation experiment LOHAFEX in the Southern Ocean, *Deep-Sea Res. Pt. I*, 89, 94–103, doi:10.1016/j.dsr.2014.04.007, 2014.

Fischer, G., Fütterer, D., Gersonde, R., Honjo, S., Ostermann, D., and Wefer, G.: Seasonal variability of particle flux in the Weddell Sea and its relation to ice cover, *Nature*, 335, 426–428, doi:10.1038/335426a0, 1988.

Fischer, G., Gersonde, R., and Wefer, G.: Organic carbon, biogenic silica and diatom fluxes in the marginal winter sea-ice zone and in the Polar Front Region: interannual variations and differences in composition, *The Southern Ocean I: Climatic Changes in the Cycle of Carbon in the Southern Ocean*, *Deep-Sea Res. Pt. II*, 49, 1721–1745, doi:10.1016/S0967-0645(02)00009-7, 2002.

Fransz, H. G. and Gonzalez, S. R.: The production of *Oithona similis* (Copepoda: Cyclopoida) in the Southern Ocean, *ICES J. Mar. Sci. J. Cons.*, 52, 549–555, doi:10.1016/1054-3139(95)80069-7, 1995.

Garrison, D. L.: Monterey Bay phytoplankton. II. Resting spore cycles in coastal diatom populations, *J. Plankton Res.*, 3, 137–156, doi:10.1093/plankt/3.1.137, 1981.

Gersonde, R. and Zielinski, U.: The reconstruction of late Quaternary Antarctic sea-ice distribution – the use of diatoms as a proxy for sea-ice, *Palaeogeogr. Palaeoclimatol.*, 162, 263–286, doi:10.1016/S0031-0182(00)00131-0, 2000.

## Export fluxes in a naturally fertilized area – Part 2

M. Rembauville et al.

Title Page

Abstract

Introduction

Conclusions

References

Tables

Figures



Back

Close

Full Screen / Esc

Printer-friendly Version

Interactive Discussion



Gleiber, M. R., Steinberg, D. K., and Ducklow, H. W.: Time series of vertical flux of zooplankton fecal pellets on the continental shelf of the western Antarctic Peninsula, *Mar. Ecol.-Prog. Ser.*, 471, 23–36, doi:10.3354/meps10021, 2012.

Gomi, Y., Fukuchi, M., and Taniguchi, A.: Diatom assemblages at subsurface chlorophyll maximum layer in the eastern Indian sector of the Southern Ocean in summer, *J. Plankton Res.*, 32, 1039–1050, doi:10.1093/plankt/fbq031, 2010.

Gonzalez, H. E. and Smetacek, V.: The possible role of the cyclopoid copepod *Oithona* in retarding vertical flux of zooplankton faecal material, *Mar. Ecol.-Prog. Ser.*, 113, 233–246, 1994.

Grigorov, I., Rigual-Hernandez, A. S., Honjo, S., Kemp, A. E. S., and Armand, L. K.: Settling fluxes of diatoms to the interior of the Antarctic circumpolar current along 170° W, *Deep-Sea Res. Pt. I*, 93, 1–13, doi:10.1016/j.dsr.2014.07.008, 2014.

Grimm, K. A., Lange, C. B., and Gill, A. S.: Biological forcing of hemipelagic sedimentary laminae; evidence from ODP Site 893, Santa Barbara Basin, California, *J. Sediment. Res.*, 66, 613–624, doi:10.1306/D42683C4-2B26-11D7-8648000102C1865D, 1996.

Hasle, G. R. and Syvertsen, E. E.: Marine diatoms, in: *Identifying Marine Phytoplankton*, chapter 2, edited by: Tomas, C. R., Academic Press, San Diego, 5–385, 1997.

Hillebrand, H., Dürselen, C.-D., Kirschtel, D., Pollinger, U., and Zohary, T.: Biovolume calculation for pelagic and benthic microalgae, *J. Phycol.*, 35, 403–424, doi:10.1046/j.1529-8817.1999.3520403.x, 1999.

Holm-Hansen, O., Kahru, M., Hewes, C. D., Kawaguchi, S., Kameda, T., Sushin, V. A., Krasovski, I., Priddle, J., Korb, R., Hewitt, R. P., and Mitchell, B. G.: Temporal and spatial distribution of chlorophyll *a* in surface waters of the Scotia Sea as determined by both shipboard measurements and satellite data, *Deep-Sea Res. Pt. II*, 51, 1323–1331, doi:10.1016/j.dsr2.2004.06.004, 2004.

Holzer, M., Primeau, F. W., DeVries, T., and Matear, R.: The Southern Ocean silicon trap: data-constrained estimates of regenerated silicic acid, trapping efficiencies, and global transport paths, *J. Geophys. Res.-Oceans*, 119, 313–331, 2013.

Howard, A. G., Coxhead, A. J., Potter, I. A., and Watt, A. P.: Determination of dissolved aluminium by the micelle-enhanced fluorescence of its lumogallion complex, *Analyst*, 111, 1379–1382, doi:10.1039/AN9861101379, 1986.

Hutchins, D. A. and Bruland, K. W.: Iron-limited diatom growth and Si:N uptake ratios in a coastal upwelling regime, *Nature*, 393, 561–564, doi:10.1038/31203, 1998.

## Export fluxes in a naturally fertilized area – Part 2

M. Rembauville et al.

Title Page

Abstract

Introduction

Conclusions

References

Tables

Figures



Back

Close

Full Screen / Esc

Printer-friendly Version

Interactive Discussion



Ichinomiya, M., Gomi, Y., Nakamachi, M., Honda, M., Fukuchi, M., and Taniguchi, A.: Temporal variations in the abundance and sinking flux of diatoms under fast ice in summer near Syowa Station, East Antarctica, *Polar Sci.*, 2, 33–40, doi:10.1016/j.polar.2008.01.001, 2008.

Jackson, G. A. and Burd, A. B.: A model for the distribution of particle flux in the mid-water column controlled by subsurface biotic interactions, the US JGOFS Synthesis and Modeling Project: Phase 1, *Deep-Sea Res. Pt. II*, 49, 193–217, doi:10.1016/S0967-0645(01)00100-X, 2001.

Jackson, G. A., Waite, A. M., and Boyd, P. W.: Role of algal aggregation in vertical carbon export during SOIREE and in other low biomass environments, *Geophys. Res. Lett.*, 32, L13607, doi:10.1029/2005GL023180, 2005.

Jin, X., Gruber, N., Dunne, J. P., Sarmiento, J. L., and Armstrong, R. A.: Diagnosing the contribution of phytoplankton functional groups to the production and export of particulate organic carbon, CaCO<sub>3</sub>, and opal from global nutrient and alkalinity distributions, *Global Biogeochem. Cy.*, 20, GB2015, doi:10.1029/2005GB002532, 2006.

Jouandet, M. P., Blain, S., Metzl, N., Brunet, C., Trull, T. W., and Obernosterer, I.: A seasonal carbon budget for a naturally iron-fertilized bloom over the Kerguelen Plateau in the Southern Ocean, KEOPS: Kerguelen Ocean and Plateau compared Study, *Deep-Sea Res. Pt. II*, 55, 856–867, doi:10.1016/j.dsr2.2007.12.037, 2008.

Jouandet, M.-P., Trull, T. W., Guidi, L., Picheral, M., Ebersbach, F., Stemmann, L., and Blain, S.: Optical imaging of mesopelagic particles indicates deep carbon flux beneath a natural iron-fertilized bloom in the Southern Ocean, *Limnol. Oceanogr.*, 56, 1130–1140, doi:10.4319/lo.2011.56.3.1130, 2011.

Kato, M., Tanimura, Y., Matsuoka, K., and Fukusawa, H.: Planktonic diatoms from sediment traps in Omura Bay, western Japan with implications for ecological and taphonomic studies of coastal marine environments, *Quatern. Int.*, 105, 25–31, doi:10.1016/S1040-6182(02)00147-7, 2003.

Kemp, A. E., Pike, J., Pearce, R. B., and Lange, C. B.: The “Fall dump” – a new perspective on the role of a “shade flora” in the annual cycle of diatom production and export flux, *Deep-Sea Res. Pt. II*, 47, 2129–2154, doi:10.1016/S0967-0645(00)00019-9, 2000.

Kemp, A. E. S. and Villareal, T. A.: High diatom production and export in stratified waters – a potential negative feedback to global warming, *Prog. Oceanogr.*, 119, 4–23, 2013.

Kohfeld, K. E., Quéré, C. L., Harrison, S. P., and Anderson, R. F.: Role of marine biology in glacial–interglacial CO<sub>2</sub> cycles, *Science*, 308, 74–78, doi:10.1126/science.1105375, 2005.

---

**Export fluxes in  
a naturally fertilized  
area – Part 2**M. Rembauville et al.

---

[Title Page](#)[Abstract](#)[Introduction](#)[Conclusions](#)[References](#)[Tables](#)[Figures](#)[Back](#)[Close](#)[Full Screen / Esc](#)[Printer-friendly Version](#)[Interactive Discussion](#)

Kuwata, A. and Tsuda, A.: Selection and viability after ingestion of vegetative cells, resting spores and resting cells of the marine diatom, *Chaetoceros pseudocurvisetus*, by two copepods, *J. Exp. Mar. Biol. Ecol.*, 322, 143–151, doi:10.1016/j.jembe.2005.02.013, 2005.

Kuwata, A., Hama, T., and Takahashi, M.: Ecophysiological characterization of two life forms, resting spores and resting cells, of a marine planktonic diatom, *Mar. Ecol.-Prog. Ser.*, 102, 245–255, 1993.

Lam, P. J. and Bishop, J. K. B.: High biomass, low export regimes in the Southern Ocean, *Deep-Sea Res. Pt. II*, 54, 601–638, doi:10.1016/j.dsr2.2007.01.013, 2007.

Lam, P. J., Doney, S. C., and Bishop, J. K. B.: The dynamic ocean biological pump: insights from a global compilation of particulate organic carbon,  $\text{CaCO}_3$ , and opal concentration profiles from the mesopelagic, *Global Biogeochem. Cy.*, 25, GB3009, doi:10.1029/2010GB003868, 2011.

Lampitt, R. S., Noji, T., and von Bodungen, B.: What happens to zooplankton faecal pellets? Implications for material flux, *Mar. Biol.*, 104, 15–23, doi:10.1007/BF01313152, 1990.

Lampitt, R. S., Boorman, B., Brown, L., Lucas, M., Salter, I., Sanders, R., Saw, K., Seeyave, S., Thomalla, S. J., and Turnewitsch, R.: Particle export from the euphotic zone: estimates using a novel drifting sediment trap,  $^{234}\text{Th}$  and new production, *Deep-Sea Res. Pt. I*, 55, 1484–1502, doi:10.1016/j.dsr.2008.07.002, 2008.

Lampitt, R. S., Salter, I., and Johns, D.: Radiolaria: Major exporters of organic carbon to the deep ocean, *Global Biogeochem. Cy.*, 23, GB1010, doi:10.1029/2008GB003221, 2009.

Lange, C. B., Weinheimer, A. L., Reid, F. M. H., and Thunell, R. C.: Sedimentation patterns of diatoms, radiolarians, and silicoflagellates in Santa Barbara Basin, California, *California Cooperative Oceanic Fisheries Investigations Reports* 38, 161–170, 1997.

Laurenceau, E. C., Trull, T. W., Davies, D. M., Bray, S. G., Doran, J., Planchon, F., Carlotti, F., Jouandet, M.-P., Cavagna, A.-J., Waite, A. M., and Blain, S.: The relative importance phytoplankton aggregates and zooplankton fecal pellets to carbon export: insights from drifting sediment trap deployments in naturally iron-fertilised waters near the Kerguelen plateau, *Biogeosciences Discuss.*, 11, 13623–13673, doi:10.5194/bgd-11-13623-2014, 2014.

Lasbleiz, M., Leblanc, K., Blain, S., Ras, J., Cornet-Barthaux, V., Hélias Nunige, S., and Quéguiner, B.: Pigments, elemental composition (C, N, P, and Si), and stoichiometry of particulate matter in the naturally iron fertilized region of Kerguelen in the Southern Ocean, *Biogeosciences*, 11, 5931–5955, doi:10.5194/bg-11-5931-2014, 2014.

## Export fluxes in a naturally fertilized area – Part 2

M. Rembauville et al.

Title Page

Abstract

Introduction

Conclusions

References

Tables

Figures



Back

Close

Full Screen / Esc

Printer-friendly Version

Interactive Discussion



- Legendre, P. and Dr, L. F. J. L.: Numerical Ecology, 2. edn., Elsevier Science, Amsterdam, New York, 1998.
- Leventer, A.: Sediment trap diatom assemblages from the northern Antarctic Peninsula region, *Deep-Sea Res. Pt. I*, 38, 1127–1143, doi:10.1016/0198-0149(91)90099-2, 1991.
- 5 Leventer, A. and Dunbar, R. B.: Diatom flux in McMurdo Sound, Antarctica, *Mar. Micropaleontol.*, 12, 49–64, doi:10.1016/0377-8398(87)90013-2, 1987.
- Lopes, C., Mix, A. C., and Abrantes, F.: Diatoms in northeast Pacific surface sediments as paleoceanographic proxies, *Mar. Micropaleontol.*, 60, 45–65, doi:10.1016/j.marmicro.2006.02.010, 2006.
- 10 Madin, L. P.: Production, composition and sedimentation of salp fecal pellets in oceanic waters, *Mar. Biol.*, 67, 39–45, doi:10.1007/BF00397092, 1982.
- Maiti, K., Charette, M. A., Buesseler, K. O., and Kahru, M.: An inverse relationship between production and export efficiency in the Southern Ocean, *Geophys. Res. Lett.*, 40, 1557–1561, doi:10.1002/grl.50219, 2013.
- 15 Martin, J. H., Gordon, R. M., and Fitzwater, S. E.: Iron in Antarctic waters, *Nature*, 345, 156–158, doi:10.1038/345156a0, 1990.
- Matsumoto, K., Sarmiento, J. L., and Brzezinski, M. A.: Silicic acid leakage from the Southern Ocean: a possible explanation for glacial atmospheric  $p\text{CO}_2$ , *Global Biogeochem. Cy.*, 16, 5–1, doi:10.1029/2001GB001442, 2002.
- 20 McQuoid, M. R. and Hobson, L. A.: Diatom resting stages, *J. Phycol.*, 32, 889–902, doi:10.1111/j.0022-3646.1996.00889.x, 1996.
- Menden-Deuer, S. and Lessard, E. J.: Carbon to volume relationships for dinoflagellates, diatoms, and other protist plankton, *Limnol. Oceanogr.*, 45, 569–579, doi:10.4319/lo.2000.45.3.0569, 2000.
- 25 Moore, C. M., Mills, M. M., Arrigo, K. R., Berman-Frank, I., Bopp, L., Boyd, P. W., Galbraith, E. D., Geider, R. J., Guieu, C., Jaccard, S. L., Jickells, T. D., La Roche, J., Lenton, T. M., Mahowald, N. M., Marañón, E., Marinov, I., Moore, J. K., Nakatsuka, T., Oschlies, A., Saito, M. A., Thingstad, T. F., Tsuda, A., and Ulloa, O.: Processes and patterns of oceanic nutrient limitation, *Nat. Geosci.*, 6, 701–710, doi:10.1038/ngeo1765, 2013.
- 30 Moore, J. K., Doney, S. C., Glover, D. M., and Fung, I. Y.: Iron cycling and nutrient-limitation patterns in surface waters of the World Ocean, *Deep-Sea Res.*, 49, 463–507, doi:10.1016/S0967-0645(01)00109-6, 2001.

## Export fluxes in a naturally fertilized area – Part 2

M. Rembauville et al.

Title Page

Abstract

Introduction

Conclusions

References

Tables

Figures



Back

Close

Full Screen / Esc

Printer-friendly Version

Interactive Discussion



Mosseri, J., Quéguiner, B., Armand, L., and Cornet-Barthaux, V.: Impact of iron on silicon utilization by diatoms in the Southern Ocean: a case study of Si/N cycle decoupling in a naturally iron-enriched area, KEOPS: Kerguelen Ocean and Plateau compared Study, *Deep-Sea Res. Pt. II*, 55, 801–819, doi:10.1016/j.dsr2.2007.12.003, 2008.

5 Nelson, D. M., Tréguer, P., Brzezinski, M. A., Leynaert, A., and Quéguiner, B.: Production and dissolution of biogenic silica in the ocean: revised global estimates, comparison with regional data and relationship to biogenic sedimentation, *Global Biogeochem. Cy.*, 9, 359–372, doi:10.1029/95GB01070, 1995.

10 Nelson, D. M., Brzezinski, M. A., Sigmon, D. E., and Franck, V. M.: A seasonal progression of Si limitation in the Pacific sector of the Southern Ocean, *Deep-Sea Res. Pt. II*, 48, 3973–3995, doi:10.1016/S0967-0645(01)00076-5, 2001.

Oku, O. and Kamatani, A.: Resting spore formation of the marine planktonic diatom *Chaetoceros anastomosans* induced by high salinity and nitrogen depletion, *Mar. Biol.*, 127, 515–520, doi:10.1007/s002270050040, 1997.

15 Park, J., Oh, I.-S., Kim, H.-C., and Yoo, S.: Variability of SeaWiFs chlorophyll *a* in the southwest Atlantic sector of the Southern Ocean: strong topographic effects and weak seasonality, *Deep-Sea Res. Pt. I*, 57, 604–620, doi:10.1016/j.dsr.2010.01.004, 2010.

20 Park, Y.-H., Roquet, F., Durand, I., and Fuda, J.-L.: Large-scale circulation over and around the Northern Kerguelen Plateau, *Deep-Sea Res. Pt. II*, 55, 566–581, doi:10.1016/j.dsr2.2007.12.030, 2008.

Park, Y.-H., Durand, I., Kestenare, E., Rougier, G., Zhou, M., d' Ovidio, F., Cotté, C., and Lee, J.-H.: Polar front around the Kerguelen Islands: an up-to-date determination and associated circulation of surface/subsurface waters, *J. Geophys. Res.-Oceans*, 119, doi:10.1002/2014JC010061, 2014.

25 Parslow, J. S., Boyd, P. W., Rintoul, S. R., and Griffiths, F. B.: A persistent subsurface chlorophyll maximum in the Interpolar Frontal Zone south of Australia: seasonal progression and implications for phytoplankton-light-nutrient interactions, *J. Geophys. Res.-Oceans*, 106, 31543–31557, doi:10.1029/2000JC000322, 2001.

30 Pilskaln, C. H., Manganini, S. J., Trull, T. W., Armand, L., Howard, W., Asper, V. L., and Massom, R.: Geochemical particle fluxes in the Southern Indian Ocean seasonal ice zone: Prydz Bay region, East Antarctica, *Deep-Sea Res. Pt. I*, 51, 307–332, doi:10.1016/j.dsr.2003.10.010, 2004.

## Export fluxes in a naturally fertilized area – Part 2

M. Rembauville et al.

[Title Page](#)

[Abstract](#)

[Introduction](#)

[Conclusions](#)

[References](#)

[Tables](#)

[Figures](#)



[Back](#)

[Close](#)

[Full Screen / Esc](#)

[Printer-friendly Version](#)

[Interactive Discussion](#)



Pinkerton, M. H., Smith, A. N. H., Raymond, B., Hosie, G. W., Sharp, B., Leathwick, J. R., and Bradford-Grieve, J. M.: Spatial and seasonal distribution of adult *Oithona similis* in the Southern Ocean: predictions using boosted regression trees, *Deep-Sea Res. Pt. I*, 57, 469–485, doi:10.1016/j.dsr.2009.12.010, 2010.

Pollard, R., Lucas, M., and Read, J.: Physical controls on biogeochemical zonation in the Southern Ocean, *Deep-Sea Res. Pt. II*, 49, 3289–3305, doi:10.1016/S0967-0645(02)00084-X, 2002.

Primeau, F. W., Holzer, M., and DeVries, T.: Southern Ocean nutrient trapping and the efficiency of the biological pump, *J. Geophys. Res.-Oceans*, 118, 2547–2564, doi:10.1002/jgrc.20181, 2013.

Quéguiner, B.: Iron fertilization and the structure of planktonic communities in high nutrient regions of the Southern Ocean, *Deep-Sea Res. Pt. II*, 90, 43–54, doi:10.1016/j.dsr2.2012.07.024, 2013.

Ragueneau, O., Savoye, N., Del Amo, Y., Cotten, J., Tardiveau, B., and Leynaert, A.: A new method for the measurement of biogenic silica in suspended matter of coastal waters: using Si : Al ratios to correct for the mineral interference, *Cont. Shelf Res.*, 25, 697–710, doi:10.1016/j.csr.2004.09.017, 2005.

Ragueneau, O., Schultes, S., Bidle, K., Claquin, P., and Moriceau, B.: Si and C interactions in the world ocean: importance of ecological processes and implications for the role of diatoms in the biological pump, *Global Biogeochem. Cy.*, 20, GB4S02, doi:10.1029/2006GB002688, 2006.

Rembauville, M., Blain, S., Armand, L., Quéguiner, B., and Salter, I.: Export fluxes in a naturally fertilized area of the Southern Ocean, the Kerguelen Plateau: seasonal dynamic reveals long lags and strong attenuation of particulate organic carbon fluxes (Part 1), *Biogeosciences Discuss.*, 11, 17043–17087, doi:10.5194/bgd-11-17043-2014, 2014.

Richardson, K., Visser, A. W., and Pedersen, F. B.: Subsurface phytoplankton blooms fuel pelagic production in the North Sea, *J. Plankton Res.*, 22, 1663–1671, doi:10.1093/plankt/22.9.1663, 2000.

Rigual-Hernandez, A. S., Trull, T. W., Bray, S. G., Closset, I., and Armand, L. K.: Seasonal dynamics in diatom and particulate export fluxes to the deep sea in the Australian sector of the southern Antarctic Zone, *J. Marine Syst.*, 142, 62–74, 2014.

## Export fluxes in a naturally fertilized area – Part 2

M. Rembauville et al.

Title Page

Abstract

Introduction

Conclusions

References

Tables

Figures



Back

Close

Full Screen / Esc

Printer-friendly Version

Interactive Discussion



Romero, O. E. and Armand, L.: Marine diatoms as indicators of modern changes in oceanographic conditions, in: *The Diatoms: Applications for the Environmental and Earth Sciences*, 2nd edn., Camb. Univ. Press, 373–400., 2010.

Romero, O. E., Lange, C. B., Fisher, G., Treppke, U. F., and Wefer, G.: Variability in export production documented by downward fluxes and species composition of marine planktonic diatoms: observations from the tropical and equatorial Atlantic, in: *The Use of Proxies in Paleoceanography, Examples from the South Atlantic*, Heidelberg, Berlin, 365–392, 1999.

Romero, O. E., Fischer, G., Lange, C. B., and Wefer, G.: Siliceous phytoplankton of the western equatorial Atlantic: sediment traps and surface sediments, *Deep-Sea Res. Pt. II*, 47, 1939–1959, doi:10.1016/S0967-0645(00)00012-6, 2000.

Rynearson, T. A., Richardson, K., Lampitt, R. S., Sieracki, M. E., Poulton, A. J., Lyngsgaard, M. M., and Perry, M. J.: Major contribution of diatom resting spores to vertical flux in the sub-polar North Atlantic, *Deep-Sea Res. Pt. I*, 82, 60–71, doi:10.1016/j.dsr.2013.07.013, 2013.

Sackett, O., Armand, L., Beardall, J., Hill, R., Doblin, M., Connelly, C., Howes, J., Stuart, B., Ralph, P., and Heraud, P.: Taxon-specific responses of Southern Ocean diatoms to Fe enrichment revealed by synchrotron radiation FTIR microspectroscopy, *Biogeosciences*, 11, 5795–5808, doi:10.5194/bg-11-5795-2014, 2014.

Sallée, J.-B., Matear, R. J., Rintoul, S. R., and Lenton, A.: Localized subduction of anthropogenic carbon dioxide in the Southern Hemisphere oceans, *Nat. Geosci.*, 5, 579–584, doi:10.1038/ngeo1523, 2012.

Salter, I., Lampitt, R. S., Sanders, R., Poulton, A., Kemp, A. E. S., Boorman, B., Saw, K., and Pearce, R.: Estimating carbon, silica and diatom export from a naturally fertilised phytoplankton bloom in the Southern Ocean using PELAGRA: a novel drifting sediment trap, *The Crozet Natural Iron Bloom and Export Experiment CROZEX*, *Deep-Sea Res. Pt. II*, 54, 2233–2259, doi:10.1016/j.dsr2.2007.06.008, 2007.

Salter, I., Kemp, A. E. S., Moore, C. M., Lampitt, R. S., Wolff, G. A., and Holtvoeth, J.: Diatom resting spore ecology drives enhanced carbon export from a naturally iron-fertilized bloom in the Southern Ocean: *Eucampia* driven carbon fluxes, *Global Biogeochem. Cy.*, 26, GB1014, doi:10.1029/2010GB003977, 2012.

Sancetta, C.: Diatoms in the Gulf of California: seasonal flux patterns and the sediment record for the last 15 000 years, *Paleoceanography*, 10, 67–84, doi:10.1029/94PA02796, 1995.

## Export fluxes in a naturally fertilized area – Part 2

M. Rembauville et al.

Title Page

Abstract

Introduction

Conclusions

References

Tables

Figures



Back

Close

Full Screen / Esc

Printer-friendly Version

Interactive Discussion



- Sanders, J. G. and Cibik, S. J.: Reduction of growth rate and resting spore formation in a marine diatom exposed to low levels of cadmium, *Mar. Environ. Res.*, 16, 165–180, doi:10.1016/0141-1136(85)90136-9, 1985.
- Sarmiento, J. L., Slater, R., Barber, R., Bopp, L., Doney, S. C., Hirst, A. C., Kleypas, J., Matear, R., Mikolajewicz, U., Monfray, P., Soldatov, V., Spall, S. A., and Stouffer, R.: Response of ocean ecosystems to climate warming, *Global Biogeochem. Cy.*, 18, GB3003, doi:10.1029/2003GB002134, 2004.
- Schnack-Schiel, S. B. and Isla, E.: The role of zooplankton in the pelagic-benthic coupling of the Southern Ocean, *Sci. Mar.*, 69, 39–55, 2005.
- Smetacek, V. S.: Role of sinking in diatom life-history cycles: ecological, evolutionary and geological significance, *Mar. Biol.*, 84, 239–251, doi:10.1007/BF00392493, 1985.
- Smetacek, V., Assmy, P., and Henjes, J.: The role of grazing in structuring Southern Ocean pelagic ecosystems and biogeochemical cycles, *Antarct. Sci.*, 16, 541–558, doi:10.1017/S0954102004002317, 2004.
- Steinberg, D. K., Goldthwait, S. A., and Hansell, D. A.: Zooplankton vertical migration and the active transport of dissolved organic and inorganic nitrogen in the Sargasso Sea, *Deep-Sea Res. Pt. I*, 49, 1445–1461, doi:10.1016/S0967-0637(02)00037-7, 2002.
- Suzuki, H., Sasaki, H., and Fukuchi, M.: Short-term variability in the flux of rapidly sinking particles in the Antarctic marginal ice zone, *Polar Biol.*, 24, 697–705, doi:10.1007/s003000100271, 2001.
- Suzuki, H., Sasaki, H., and Fukuchi, M.: Loss processes of sinking fecal pellets of zooplankton in the mesopelagic layers of the Antarctic marginal ice zone, *J. Oceanogr.*, 59, 809–818, doi:10.1023/B:JOCE.0000009572.08048.0d, 2003.
- Takahashi, T., Sweeney, C., Hales, B., Chipman, D., Newberger, T., Goddard, J., Iannuzzi, R., and Sutherland, S.: The changing carbon cycle in the Southern Ocean, *Oceanography*, 25, 26–37, doi:10.5670/oceanog.2012.71, 2012.
- Takeda, S.: Influence of iron availability on nutrient consumption ratio of diatoms in oceanic waters, *Nature*, 393, 774–777, doi:10.1038/31674, 1998.
- Tarling, G. A., Ward, P., Atkinson, A., Collins, M. A., and Murphy, E. J.: DISCOVERY 2010: spatial and temporal variability in a dynamic polar ecosystem, *Deep-Sea Res. Pt. II*, 59–60, 1–13, doi:10.1016/j.dsr2.2011.10.001, 2012.
- Taylor, S. R. and McClennan, S. M.: The continental crust: its composition and evolution, *Geol. J.* 21, 85–86, doi:10.1002/gj.3350210116, 1986.

---

**Export fluxes in  
a naturally fertilized  
area – Part 2**M. Rembauville et al.

---

[Title Page](#)[Abstract](#)[Introduction](#)[Conclusions](#)[References](#)[Tables](#)[Figures](#)[Back](#)[Close](#)[Full Screen / Esc](#)[Printer-friendly Version](#)[Interactive Discussion](#)

Thomalla, S. J., Fauchereau, N., Swart, S., and Monteiro, P. M. S.: Regional scale characteristics of the seasonal cycle of chlorophyll in the Southern Ocean, *Biogeosciences*, 8, 2849–2866, doi:10.5194/bg-8-2849-2011, 2011.

Treppke, U. F., Lange, C. B., and Wefer, G.: Vertical fluxes of diatoms and silicoflagellates in the eastern equatorial Atlantic, and their contribution to the sedimentary record, *Mar. Micropaleontol.*, 28, 73–96, doi:10.1016/0377-8398(95)00046-1, 1996.

Uitz, J., Claustre, H., Griffiths, F. B., Ras, J., Garcia, N., and Sandroni, V.: A phytoplankton class-specific primary production model applied to the Kerguelen Islands region (Southern Ocean), *Deep-Sea Res. Pt. I*, 56, 541–560, doi:10.1016/j.dsr.2008.11.006, 2009.

Venables, H. and Moore, C. M.: Phytoplankton and light limitation in the Southern Ocean: learning from high-nutrient, high-chlorophyll areas, *J. Geophys. Res.-Oceans*, 115, C02015, doi:10.1029/2009JC005361, 2010.

von Bodungen, B.: Phytoplankton growth and krill grazing during spring in the Bransfield Strait, Antarctica – implications from sediment trap collections, *Polar Biol.*, 6, 153–160, doi:10.1007/BF00274878, 1986.

Von Bodungen, B., Fischer, G., Nöthig, E.-M., and Wefer, G.: Sedimentation of krill faeces during spring development of phytoplankton in Bransfield Strait, Antarctica, *Mitt Geol Paläont Inst Univ Hambg. SCOPEUNEP Sonderbd*, 62, 243–257, 1987.

Weber, T. S. and Deutsch, C.: Ocean nutrient ratios governed by plankton biogeography, *Nature*, 467, 550–554, doi:10.1038/nature09403, 2010.

Wefer, G. and Fischer, G.: Annual primary production and export flux in the Southern Ocean from sediment trap data, biochemistry and circulation of water masses in the Southern Ocean International Symposium, *Mar. Chem.*, 35, 597–613, doi:10.1016/S0304-4203(09)90045-7, 1991.

Wefer, G., Fischer, G., Fütterer, D., and Gersonde, R.: Seasonal particle flux in the Bransfield Strait, Antarctica, *Deep-Sea Res. Pt. I*, 35, 891–898, doi:10.1016/0198-0149(88)90066-0, 1988.

Wefer, G. G., Fisher, D. K., Fütterer, R., Gersonde, R., Honjo, S., and Ostermann, D.: Particle sedimentation and productivity in Antarctic waters of the Atlantic sector, in: *Geological History of the Polar Oceans: Arctic vs. Antarctic*, Kluwer Academic Publishers, the Netherlands, 363–379, 1990.

## Export fluxes in a naturally fertilized area – Part 2

M. Rembauville et al.

Title Page

Abstract

Introduction

Conclusions

References

Tables

Figures



Back

Close

Full Screen / Esc

Printer-friendly Version

Interactive Discussion



Westberry, T. K., Behrenfeld, M. J., Milligan, A. J., and Doney, S. C.: Retrospective satellite ocean color analysis of purposeful and natural ocean iron fertilization, *Deep-Sea Res. Pt. I*, 73, 1–16, doi:10.1016/j.dsr.2012.11.010, 2013.

Wilson, S. E., Steinberg, D. K., and Buesseler, K. O.: Changes in fecal pellet characteristics with depth as indicators of zooplankton repackaging of particles in the mesopelagic zone of the subtropical and subarctic North Pacific Ocean, *Deep-Sea Res. Pt. II*, 55, 1636–1647, doi:10.1016/j.dsr2.2008.04.019, 2008.

Wilson, S., E., Ruhl, H. A., and Smith Jr, K. L.: Zooplankton fecal pellet flux in the abyssal northeast Pacific: a 15 year time-series study, *Limnol. Oceanogr.*, 58, 881–892, doi:10.4319/lo.2013.58.3.0881, 2013.

Wolff, E. W., Fischer, H., Fundel, F., Ruth, U., Twarloh, B., Littot, G. C., Mulvaney, R., Röthlisberger, R., de Angelis, M., Boutron, C. F., Hansson, M., Jonsell, U., Hutterli, M. A., Lambert, F., Kaufmann, P., Stauffer, B., Stocker, T. F., Steffensen, J. P., Bigler, M., Siggaard-Andersen, M. L., Udisti, R., Becagli, S., Castellano, E., Severi, M., Wagenbach, D., Barbante, C., Gabrielli, P., and Gaspari, V.: Southern Ocean sea-ice extent, productivity and iron flux over the past eight glacial cycles, *Nature*, 440, 491–496, doi:10.1038/nature04614, 2006.

Yoon, W., Kim, S., and Han, K.: Morphology and sinking velocities of fecal pellets of copepod, molluscan, euphausiid, and salp taxa in the northeastern tropical Atlantic, *Mar. Biol.*, 139, 923–928, doi:10.1007/s002270100630, 2001.

Zielinski, U. and Gersonde, R.: Diatom distribution in Southern Ocean surface sediments (Atlantic sector): implications for paleoenvironmental reconstructions, *Palaeogeogr. Palaeoclimatol.*, 129, 213–250, doi:10.1016/S0031-0182(96)00130-7, 1997.



## Export fluxes in a naturally fertilized area – Part 2

M. Rembauville et al.

[Title Page](#)

[Abstract](#)

[Introduction](#)

[Conclusions](#)

[References](#)

[Tables](#)

[Figures](#)



[Back](#)

[Close](#)

[Full Screen / Esc](#)

[Printer-friendly Version](#)

[Interactive Discussion](#)



**Table 2.** *Chaetoceros* resting spores (CRS) and *Thalassiosira antarctica* resting spores (TRS) measurement and biomass data from station A3 sediment trap covering cups #4 (December 2011) to #11 (April 2012). For each variable, the range and the mean value (**bold**) is reported.

Spore type	Number measured	Pervalvar axis ( $\mu\text{m}$ )	Apical axis ( $\mu\text{m}$ )	Shape <sup>a</sup>	Cell volume ( $\mu\text{m}^3$ )	Volume/Carbon relationship	Cell carbon content ( $\text{pmol C cell}^{-1}$ )	Cell carbon content ( $\text{pg C cell}^{-1}$ )
CRS	63	3.1–8.5	7.2–17.4	Cylinder + two cones	116.9–1415	$0.039 \text{ pmol C } \mu\text{m}^{-3\text{b}}$	5–55	55–662
		<b>6</b>	<b>12.1</b>		<b>483</b>		<b>19</b>	<b>227</b>
TRS	57	10.2–26	25.6–35.3	Cylinder + two half sphere	14 035–48 477	$C = 10^{(0.811 \log_{10}(V)) - 0.541\text{c}}$	56–153	672–1839
		<b>20.8</b>	<b>32.6</b>		<b>35 502</b>		<b>119</b>	<b>1428</b>

<sup>a</sup> As defined in Hillebrand et al. (1999).

<sup>b</sup> Data representative of *Chaetoceros pseudocurvisetus* resting spore (Kuwata et al., 1993).

<sup>c</sup> Equation from Menden-Deuer and Lessard (2000), where  $C$  is the carbon content ( $\text{pg C}$ ) and  $V$  is the cell volume ( $\mu\text{m}^3$ ).



Export fluxes in  
a naturally fertilized  
area – Part 2

M. Rembauville et al.

Title Page

Abstract

Introduction

Conclusions

References

Tables

Figures

◀

▶

◀

▶

Back

Close

Full Screen / Esc

Printer-friendly Version

Interactive Discussion



**Table 4.** Full and empty diatoms cells flux ( $10^6 \text{ m}^{-2} \text{ d}^{-1}$ ) from the station A3 sediment trap. Full cells of *Chaetoceros Hyalochaete* spp. were only found as resting spores.

Species – taxa group/ Cup Number	Full cells											
	1	2	3	4	5	6	7	8	9	10	11	12
<i>Asteromphalus</i> spp.	0	0.01	0	0.03	0	0	0	0	0.12	0	0	0
<i>Chaetoceros atlanticus</i>	0	0	0	0	0	0	0	0	0.07	0	0	0
<i>Chaetoceros atlanticus f. bulbosum</i>	0	0	0	0	0	0	0	0	0	0	0	0
<i>Chaetoceros decipiens</i>	0	0	0.02	0	0	0	0	0	0.07	0	0	0
<i>Chaetoceros dichaeata</i>	0	0	0	0.07	0	0	0	0	0.26	0	0	0
<i>Chaetoceros Hyalochaete</i> spp.	0.70	0	1.95	39.92	7.42	23.04	14.37	15.88	78.29	20.24	0.68	0
<i>Corethron inerme</i>	0	0	0	0	0	0	0	0	0.23	0	0	0
<i>Corethron pennatum</i>	0	0	0	0	0	0	0	0	0	0	0	0
<i>Dactylosolen antarcticus</i>	0	0	0	0.05	0	0	0	0	0.02	0	0	0
<i>Eucampia antarctica var. antarctica</i>	0.08	0.03	0.06	0.19	0.08	0.36	0.19	0.65	1.03	0.45	0.08	0.01
<i>Fragilariopsis kerguelensis</i>	0.88	1.06	0	1.93	0.40	0.13	0.21	0.12	1.40	0	0	0
<i>Fragilariopsis separanda/rhombica</i>	0.02	0.16	0	0.68	0.05	0.20	0.13	0.07	1.47	0	0	0
<i>Guinardia cylindrus</i>	0	0	0	0	0	0	0	0	0.07	0	0	0
<i>Leptocylindrus</i> sp.	0	0	0	0.03	0	0	0	0	0	0	0	0
<i>Membraneis</i> spp.	0.04	0.01	0	0.19	0	0	0.02	0.02	0.02	0	0	0
<i>Navicula</i> spp.	0	0	0.04	0.64	0	0	0	0.29	0.58	0	0	0
<i>Odontella weissflogii</i>	0	0	0	0.08	0	0	0	0	0.05	0	0	0
<i>Pleurosigma</i> spp.	0.01	0	0	0.22	0.02	0.02	0	0.03	0.96	0.04	0	0
<i>Proboscia alata</i>	0	0	0	0	0	0	0	0	0.09	0	0	0
<i>Proboscia inermis</i>	0	0	0	0.03	0	0	0	0	0.33	0	0	0
<i>Proboscia truncata</i>	0	0	0	0	0	0	0	0	0	0	0	0
<i>Pseudo-nitzschia</i> spp.	0.26	0.02	0.21	1.81	0.08	0.45	1.85	1.56	7.08	0.36	0.02	0
<i>Rhizosolenia antennata/styliformis</i>	0	0	0	0	0	0	0	0	0.05	0	0	0
<i>Rhizosolenia chunii</i>	0	0	0	0	0.05	0	0	0.03	0.07	0	0	0
<i>Rhizosolenia crassa</i>	0	0	0	0	0	0	0	0	0	0	0	0
<i>Rhizosolenia simplex</i>	0	0	0	0	0	0	0	0	0.07	0	0	0
<i>Thalassionema nitzschioides</i> spp.	1.45	1.48	0.20	4.65	0.28	0.14	0.34	0.72	0.89	0.14	0.05	0.01
<i>Thalassiosira lentiginosa</i>	0.01	0	0	0	0	0	0	0	0	0	0	0
<i>Thalassiosira</i> spp.	0	0.05	0	0.05	0	0	0	0	0.12	0.05	0	0
<i>Thalassiosira antarctica</i> resting spore (TRS)	0.04	0	2.19	2.65	0.17	0.14	0.13	0.14	0.12	0	0.01	0
<i>Thalassiothrix antarctica</i>	0	0	0	0.02	0.05	0.04	0.34	0.14	0.70	0	0	0
<i>Small centrics</i> (< 20 $\mu\text{m}$ )	0.05	0	0	0.41	0	0	0	0	0.19	0.18	0	0
<i>Large centrics</i> (> 20 $\mu\text{m}$ )	0	0	0.05	0.08	0	0	0	0	0.05	0	0	0
Total cells	35.39	28.20	47.18	537.38	85.85	245.20	175.89	196.56	943.88	214.65	8.46	0.22

## Export fluxes in a naturally fertilized area – Part 2

M. Rembauville et al.

Table 4. Continued.

Species – taxa group/ Cup Number	Empty Cells											
	1	2	3	4	5	6	7	8	9	10	11	12
<i>Asteromphalus</i> spp.	0.02	0.02	0.09	0.08	0	0.05	0	0.03	0.05	0	0	0
<i>Chaetoceros atlanticus</i>	0	0	0	0	0	0	0	0	0	0	0	0
<i>Chaetoceros atlanticus f. bulbosum</i>	0.01	0	0	0	0	0	0	0.02	0	0.02	0	0
<i>Chaetoceros decipiens</i>	0	0	0.02	0.24	0	0	0	0	0	0	0	0
<i>Chaetoceros dichchaeta</i>	0	0	0.06	0.07	0	0	0	0	0.05	0	0.01	0
<i>Chaetoceros Hyalochaete</i> spp.	0	0	0.45	38.19	0	0	0	0.60	18.23	0.18	0	0
<i>Corethron inerme</i>	0.01	0.01	0.04	0	0	0.02	0	0	0.23	0.31	0.06	0
<i>Corethron pennatum</i>	0	0	0.02	0	0	0	0	0.02	0	0	0.01	0
<i>Dactyliosolen antarcticus</i>	0	0	0	0.05	0	0	0	0.07	0.02	0.05	0	0
<i>Eucampia antarctica var. antarctica</i>	0	0	0.04	0.25	0.06	0.05	0.06	0.09	0.28	0.11	0.04	0
<i>Fragilariopsis kerguelensis</i>	2.25	0.46	0.84	1.02	0.26	0.63	0.88	1.17	1.17	1.45	0.16	0.03
<i>Fragilariopsis separanda/rhombica</i>	0.19	0.17	0.18	0.53	0.14	0.52	0.32	0.87	0.82	1.23	0.15	0
<i>Guinardia cylindrus</i>	0	0	0	0	0	0	0	0	0	0	0	0
<i>Leptocylindrus</i> sp.	0	0	0	0	0	0	0	0	0	0	0	0
<i>Membraneis</i> spp.	0	0	0.02	0.05	0.02	0.04	0.02	0.07	0.14	0.07	0.01	0
<i>Navicula</i> spp.	0	0	0.13	0.36	0	0	0	0.12	0.12	0	0	0
<i>Odontella weissflogii</i>	0	0	0.02	0.10	0	0	0	0.02	0	0.02	0	0
<i>Pleurosigma</i> spp.	0.18	0.06	0.08	0.41	0.08	0	0.09	0.12	0.93	0.38	0.03	0
<i>Proboscia alata</i>	0	0	0	0	0	0	0	0.03	0.05	0.34	0.01	0
<i>Proboscia inermis</i>	0	0	0.01	0.08	0	0	0	0.03	0.05	0.13	0.01	0
<i>Proboscia truncata</i>	0	0	0.02	0	0	0	0	0	0	0.02	0	0
<i>Pseudo-nitzschia</i> spp.	0.59	0	0.12	0.59	0.09	0.04	0.99	0.75	5.26	0.34	0.02	0
<i>Rhizosolenia antennata/styliformis</i>	0	0	0	0	0	0	0	0.02	0.02	0.13	0	0
<i>Rhizosolenia chunii</i>	0	0	0	0.03	0	0	0	0.02	0.02	0.20	0.02	0
<i>Rhizosolenia crassa</i>	0	0	0	0	0	0	0	0	0	0.04	0	0
<i>Rhizosolenia simplex</i>	0	0	0	0	0	0	0	0.02	0	0	0	0
<i>Thalassionema nitzschioides</i> spp.	4.33	1.97	5.39	2.07	0.19	0.09	0.47	0.12	0.72	0.18	0.03	0.01
<i>Thalassiosira lentiginosa</i>	0.25	0.06	0.10	0	0	0	0	0	0	0	0	0
<i>Thalassiosira</i> spp.	0.02	0.06	0.01	0	0	0	0	0	0	0	0	0
<i>Thalassiosira antarctica</i> resting spore (TRS)	0	0	0	0	0	0	0	0	0	0	0	0
<i>Thalassiothrix antarctica</i>	0	0	0	0	0	0.02	0	0	0	0.04	0	0
<i>Small centrics</i> (< 20 µm)	0.48	0.44	2.96	16.87	0.28	0.13	0.17	0.24	0.65	0.20	0.03	0.02
<i>Large centrics</i> (> 20 µm)	0	0.03	0.01	0.20	0	0	0	0	0.16	0.04	0	0
Total cells	8.34	3.28	10.57	61.20	1.12	1.59	3.01	4.43	28.98	5.46	0.59	0.07

Title Page

Abstract

Introduction

Conclusions

References

Tables

Figures

◀

▶

◀

▶

Back

Close

Full Screen / Esc

Printer-friendly Version

Interactive Discussion







## Export fluxes in a naturally fertilized area – Part 2

M. Rembauville et al.

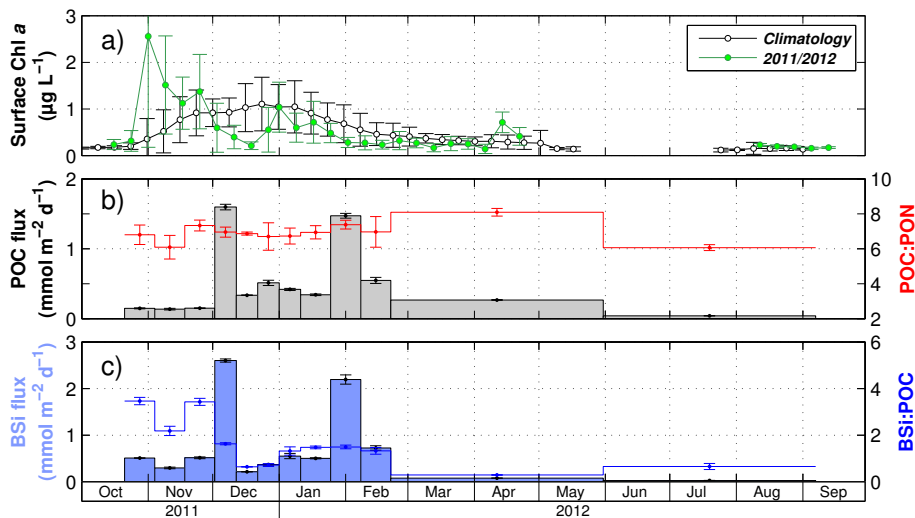


**Figure 1.** (a) Time series of the surface chlorophyll *a* concentration averaged in a 100 km radius around the trap location. (b) POC fluxes (grey bars) and C/N molar ratio (red line) of the exported material, (c) BSi flux (light blue bars) and BSi:POC ratio (blue line). Errorbars are SD on triplicates.

Title Page

Abstract

Introduction

Conclusions

References

Tables

Figures



Back

Close

Full Screen / Esc

Printer-friendly Version

Interactive Discussion



Export fluxes in  
a naturally fertilized  
area – Part 2

M. Rembauville et al.

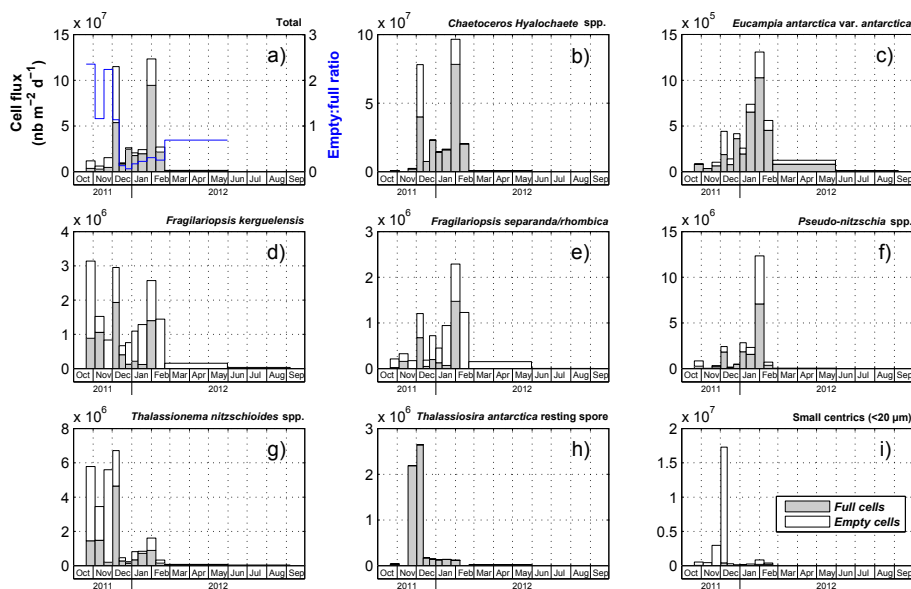


**Figure 2.** (a) Total diatom cells fluxes (bars, left axis) and total empty : full cells ratio (blue line, right axis). (b) to (h) Fluxes of diatom cells from selected species identified as major contributors to diatom fluxes (> 1 % of total diatom fluxes). In (b), full cells are *Chaetoceros Hyalochaete* resting spores and empty cells are the vegetative stage. Full cell fluxes are represented by grey bars whereas empty cell fluxes are represented by white bars

Title Page

Abstract Introduction

Conclusions References

Tables Figures

◀ ▶

◀ ▶

Back Close

Full Screen / Esc

Printer-friendly Version

Interactive Discussion



Export fluxes in  
a naturally fertilized  
area – Part 2

M. Rembauville et al.

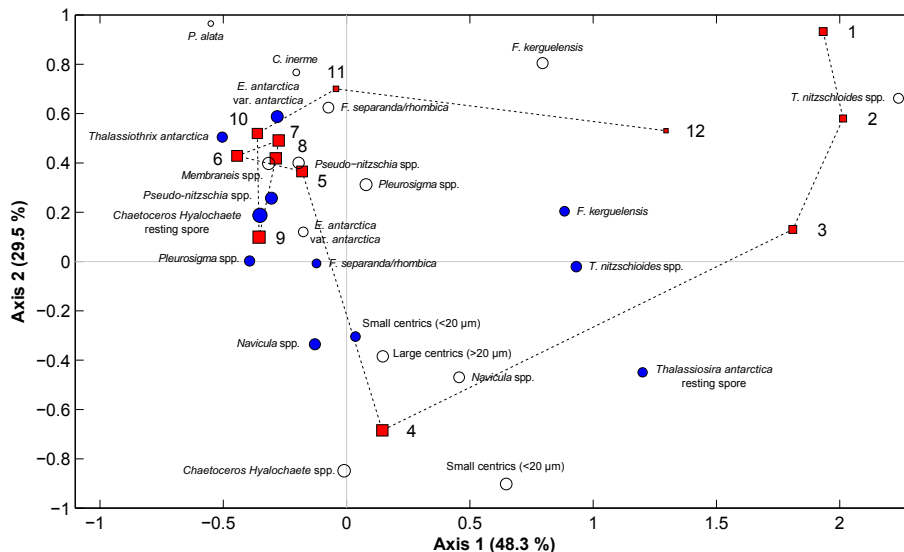


**Figure 3.** Factorial map constituted by the first two axes of the correspondence analysis performed on the full and empty diatom cell fluxes. Red squares are cup projections with cup numbers specified, blue circles are full cell projections, white circles are empty cell projections. The size of the markers is proportional to their representation quality in this factorial map.

Title Page

Abstract

Introduction

Conclusions

References

Tables

Figures



Back

Close

Full Screen / Esc

Printer-friendly Version

Interactive Discussion



## Export fluxes in a naturally fertilized area – Part 2

M. Rembauville et al.

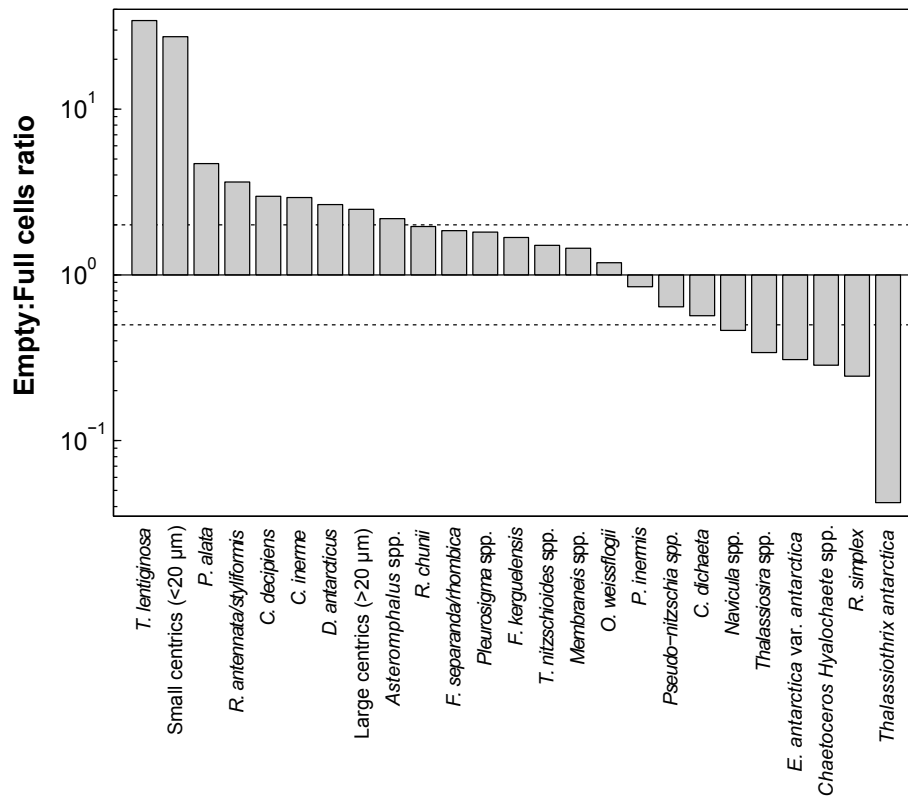


**Figure 4.** Annual ratio of empty to full cells for species observed as both forms. The dashed lines are the 0.5 and 2 ratio values. *Chaetoceros Hyalochoæte* spp. full cells were only observed as resting spores.

Title Page

Abstract

Introduction

Conclusions

References

Tables

Figures



Back

Close

Full Screen / Esc

Printer-friendly Version

Interactive Discussion



## Export fluxes in a naturally fertilized area – Part 2

M. Rembauville et al.

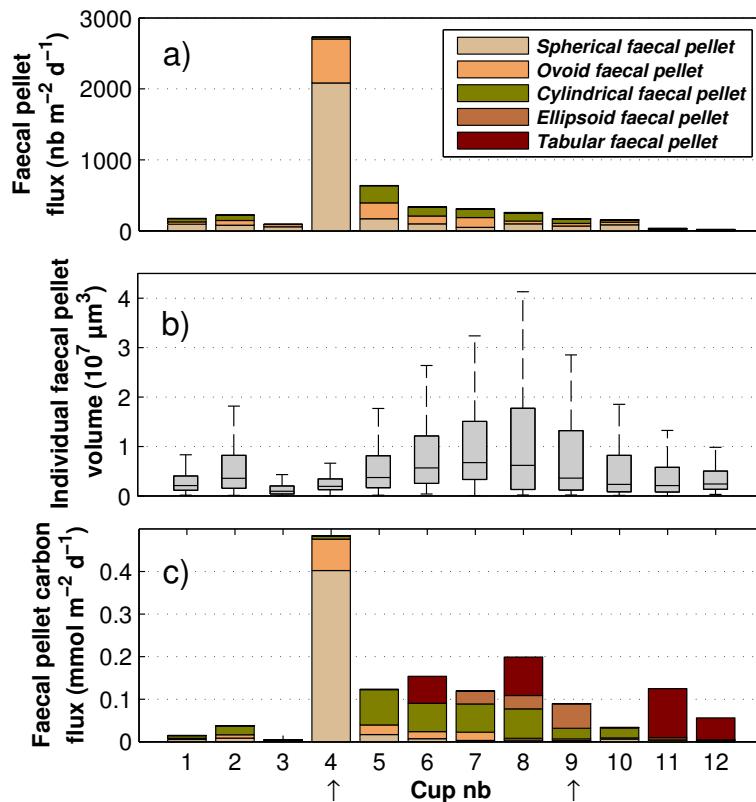


**Figure 5.** (a) Faecal pellet numerical fluxes partitioned among faecal pellet types, (b) boxplot of faecal pellet volume. On each box, the central mark is the median, the edges of the box are the first and third quartiles, the whiskers extend to the most extreme data points comprised in 1.5 times the interquartile distance. (c) Faecal pellet carbon fluxes partitioned between the five faecal pellet types. The two arrows represent the two strong POC export events (cup #4 and #9).

Export fluxes in  
a naturally fertilized  
area – Part 2

M. Rembauville et al.

		POC	PON	BSi	POC:PON	BSi:POC
①	CRS	0.07	0.07	0.06	0.02	-0.04
②	<i>E. antarctica</i>	0.05	0.05	0.03	0.02	-0.04
③	<i>F. kerguelensis</i>	0.05	0.05	0.07	0	0.07
④	<i>F. separanda/rhombica</i>	0.06	0.06	0.06	0.02	-0.01
⑤	<i>Navicula</i> spp.	0.07	0.07	0.07	0.02	0
⑥	<i>Pleurosigma</i> spp.	0.06	0.06	0.05	0.02	-0.01
⑦	<i>Pseudo-nitzschia</i> spp.	0.06	0.05	0.05	0.02	-0.01
⑧	<i>T. nitzschioides</i> spp.	0.04	0.04	0.06	0	0.07
⑨	TRS	0.03	0.03	0.05	-0.01	0.1
⑩	<i>Thalassiothrix antarctica</i>	0.04	0.04	0.03	0.01	-0.03
⑪	Small centrics (<20 $\mu$ m)	0.06	0.06	0.07	0.01	0.01
①	<i>Chaetoceros Hyalochaete</i> spp.	0.07	0.07	0.07	0.02	0
②	<i>C. inermis</i>	0.03	0.03	0.02	0.01	-0.03
③	<i>E. antarctica</i>	0.08	0.07	0.06	0.02	-0.04
④	<i>F. kerguelensis</i>	0	0.01	0.05	-0.02	0.17
⑤	<i>F. separanda/rhombica</i>	0.04	0.04	0.03	0.01	-0.03
⑥	<i>Membraneis</i> spp.	0.06	0.06	0.05	0.02	-0.04
⑦	<i>Navicula</i> spp.	0.05	0.05	0.06	0.01	0.05
⑧	<i>Pleurosigma</i> spp.	0.06	0.06	0.06	0.01	0.01
⑨	<i>P. alata</i>	0.01	0.01	0	0.01	-0.03
⑩	<i>Pseudo-nitzschia</i> spp.	0.05	0.05	0.05	0.01	0
⑪	<i>T. nitzschioides</i> spp.	-0.03	-0.02	0.04	-0.04	0.24
⑫	<i>T. lentiginosa</i>	-0.04	-0.04	0.02	-0.04	0.22
⑬	Small centrics (<20 $\mu$ m)	0.05	0.05	0.06	0.01	0.04
⑭	Large centrics (>20 $\mu$ m)	0.07	0.07	0.07	0.02	0.01
Ⓢ	Spherical faecal pellet	0.05	0.05	0.05	0.01	0.01
Ⓣ	Ovoid faecal pellet	0.05	0.05	0.04	0.01	-0.02
Ⓝ	Cylindrical faecal pellet	0	0	-0.02	0.01	-0.08
Ⓞ	Ellipsoid faecal pellet	0.03	0.03	0.01	0.01	-0.06
Ⓟ	Tabular faecal pellet	-0.01	-0.01	-0.05	0.02	-0.15

**Figure 6.** Heatmap representation of  $\beta$  correlation coefficients between the biological variables (empty and full-cell diatom and faecal pellet type fluxes) and the chemical variables (POC, PON, BSi, POC : PON and BSi : POC) resulting from the partial least square regression. Blue circles represent full diatom cells, white circles are empty diatom cells. Brown circles represent the faecal pellet type fluxes. The numbered and alphabetical labels within the symbols are used to identify the variable projections shown in Fig. 7. CRS: *Chaetoceros Hyalochaete* resting spores, TRS: *Thalassiosira antarctica* resting spores.

Title Page

Abstract

Introduction

Conclusions

References

Tables

Figures



Back

Close

Full Screen / Esc

Printer-friendly Version

Interactive Discussion





## Export fluxes in a naturally fertilized area – Part 2

M. Rembauville et al.

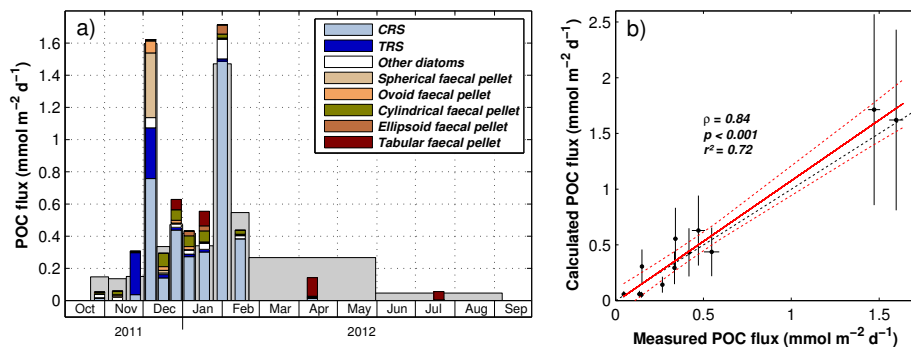


**Figure 8.** (a) Grey bars in the background are measured POC fluxes, colored bars in the foreground are calculated POC fluxes partitioned among the main ecological vectors identified. (b) Regression ( $r^2 = 0.72$ ) between the measured and calculated POC fluxes. The correlation is highly significant (Spearman rank correlation,  $n = 36$ ,  $\rho = 0.84$ ,  $p < 0.001$ ). Error bars were generated by increasing/decreasing the carbon/volume conversion factors by 50%. Black dashed line is the 1 : 1 relation, red line is the regression line, red dashed lines denotes the 99% confidence interval. CRS: *Chaetoceros Hyalochaete* resting spores, TRS: *Thalassiosira antarctica* resting spores.